

ALGEBRAIC AND COMBINATORIAL APPLICATIONS IN SYSTEMS
AND EVOLUTIONARY BIOLOGY

A DISSERTATION SUBMITTED TO THE GRADUATE DIVISION OF
THE UNIVERSITY OF HAWAII AT MĀNOA IN PARTIAL
FULFILLMENT OF THE REQUIREMENTS FOR THE DEGREE OF

DOCTOR OF PHILOSOPHY

IN

MATHEMATICS

May 2024

By

Maize Curiel

Dissertation Committee:

Elizabeth Gross, Chairperson

Bjørn Kjos-Hanssen

Chuang Xu

Vasu Tewari

June Zhang

Dedication

For all my neurodivergent queer people of color.

Acknowledgements

I would like to thank my advisor Elizabeth Gross for being an incredible mentor for the past seven years. Your guidance has lead me along the exact path that I envisioned as a graduate student and more.

Abstract

Many real-world problems can be expressed as the solution set of polynomial equations. Under these constraints, these problems are addressed using tools from (computational) algebraic geometry, commutative algebra, and combinatorics. Inspired by questions in systems and evolutionary biology, three algebraic problems are addressed in this thesis: steady-state analysis of mass-action ordinary differential equations given by directed graphs, optimal phylogenetic consensus trees, and singularities arising from linear structural equation models given by acyclic mixed graphs. Specifically, for the first algebraic problem, we introduce a polyhedral geometry tool called a mixed volume to study the steady-state degree of partitionable binomial chemical reaction networks. For the second algebraic problem, a phylogenetic consensus tree is the optimal point of a minimization problem, or a point belonging to a tropical variety, and tools from tropical combinatorics are used to locate these optimal points. For the final algebraic problem, the main object of study is the covariance parameterization map arising from linear structural equation models given by an acyclic mixed graph. The concern is with understanding the parameters for which the covariance map fails to be locally injective.

Contents

1	Introduction	1
1.1	Ideals and Varieties	4
1.2	Polyhedral Geometry	7
1.3	Zero-dimensional Solution Sets	10
2	Biological Models	16
2.1	Chemical Reaction Networks	16
2.2	Phylogenetic Trees	22
2.3	Linear Structural Equation Models	28
3	Steady-state Degree of Chemical Reaction Networks	35
3.1	Introduction	35
3.2	Mixed Volumes of Partitionable Binomial Networks	37
3.3	Cycles with Binomial Steady-States	46
4	Weighted Tropical Fermat-Weber Points	55
4.1	Introduction	55
4.1.1	Tropical polynomials and regular subdivisions	56
4.1.2	Fermat-Weber problems	64

4.1.3	Tropical convexity	68
4.2	Solving the Weighted Tropical Fermat-Weber Problem	71
4.2.1	Containment of weighted Fermat-Weber points	71
4.2.2	Any cell can be the weighted Fermat-Weber cell	72
5	Singular Locus of Linear Structural Equation Models	76
5.1	Introduction	76
5.2	Singular Locus Formulas	77
5.3	Bidirected edges	86
5.3.1	Injective does not imply monomial singular locus	89
5.3.2	Monomial singular locus does not imply injective	90
5.3.3	Relationship between singular locus term in ω and injectivity	91

List of Figures

1.1	A variety shown as the four point intersection of two hyper-surfaces, a circle and a hyperbola.	5
1.2	Illustration of the square polytope from Example 1.10.	8
1.3	The cross polytope P (top left), a trapezoid Q (top right), and their Minkowski sum (bottom).	10
1.4	A mixed subdivision (bottom) of the cross polytope (top left) and a trapezoid (top left).	15
2.1	A cyclic chemical reaction network with three species and three reactions.	17
2.2	Two phylogenetic tree on four taxa A , B , C , and D	23
2.3	A star graph on four vertices with two directed edges and a single bidirected edge.	30
3.1	A four-cycle with positive binomial steady-states.	50
4.1	The graph of $f(x) = 1 \oplus 3 \odot x \oplus -1 \odot x^{\sqrt{2}}$. The connection to the Newton polytope of f is explained in 4.1.1.	59
4.2	Left: A lift of $2\Delta^2 = \text{Newt}(f)$ with weights given by the coefficients of f , overlaid with $\text{tropV}(f)$ in black; right: $\text{tropV}(f)$	63

4.3	Subdivisions with weightings. Clockwise starting on top left: Two tropical hyperplanes in \mathbb{TR}^2 , the corresponding regular subdivision of $\Delta^1 \times \Delta^2$, the corresponding mixed subdivision of $(w_1+w_2)\Delta^2$ (weighted FW problem), and the corresponding mixed subdivision of $2\Delta^2$ (unweighted FW problem).	69
4.4	The tropical line segment between $v_1 = (0,0,0)$ and $v_2 =$ $(1,-1,0)$	70
4.5	Vertices in the product of simplices (left) correspond to the color-coded edges of the bipartite graph (right).	73

List of Tables

1.1	Summary table of problems addressed in this thesis and the corresponding tools used in the respective setting.	2
-----	--	---

Chapter 1

Introduction

The field of applied algebraic geometry studies applied problems from the lens of algebra, geometry, and combinatorics. For example, in algebraic statistics, statistical models are viewed as algebraic varieties and questions regarding inference and estimation are addressed using tools from computational algebraic geometry [28, 33]. In algebraic systems biology, both complex and real algebraic geometry are used in steady-state analysis of ODE models [6, 11]. In this dissertation, we look at three problems motivated from biology from the angle of applied algebraic geometry. In each of these problems, we use a different tool popular in applied algebraic geometry to tackle the question at hand, see Table 1.1.

The first problem investigated in this thesis is concerned with steady-state analysis of mass-action systems arising from a chemical reaction network. For more details on the biological and mathematical background in this setting see [11] or peek ahead to Section 2.1. There we introduce chemical reaction networks and the polynomial ODEs that arise. In particular, the interest is

in the so called *steady-state degree* of a chemical reaction network, which is a measure of the algebraic complexity of solving for the steady-states of the corresponding ODEs [12, 22, 27]. To get a handle on the steady-state degree of a chemical reaction network, a tool from polyhedral geometry is used. The mixed volume of a system of polynomial equations bounds its degree, that is, its number of complex solutions for generic parameters [21]. In Chapter 3, we specialize our focus to chemical reaction networks called partitionable binomial networks and our main theorem states that computing a mixed volume for these networks amounts to a calculating a matrix determinant. We then apply this result to a family of cyclic networks and show that the mixed volume depends on the parity of the number of complexes in the cycle.

Problem	Tool/Theory
Steady-state analysis	Mixed volume
Tree reconstruction	Tropical combinatorics
Identifiability of SEMs	Combinatorial matrix theory

Table 1.1: Summary table of problems addressed in this thesis and the corresponding tools used in the respective setting.

In Chapter 4, we study a phylogenetic tree reconstruction problem through the lens of tropical combinatorics which combines tropical geometry, polyhedral geometry, and combinatorics [23, 24, 36]. In Section 2.2, we introduce the space of phylogenetic trees on m leaves as a tropical linear subspace of $\mathbb{R}^{\binom{m}{2}}/\mathbb{R}\mathbb{1}$ and show an example of how tropical combinatorics can be a powerful tool for phylogenetic tree reconstruction, specifically for computing phylogenetic consensus trees. In this setting, a consensus tree is the optimal solution of an optimization problem. These optimal points are called Fermat-Weber points due to their connection to finding geometric medians of a high

dimensional data set [4, 13]. The authors of [5] show that Fermat-Weber points correspond to points belonging to the central cell of a subdivision of a certain polytope. Our main result states that when weights are included in this optimization problem, the Fermat-Weber points correspond to different cells of the same polytope. Thus, the work here generalizes the investigations of Comănesci and Joswig in [5].

The final problem investigated in this thesis deals with non-identifiable parameters of linear structural equation models. For a background on linear structural equation models see Section 2.3. The reader can also choose to refer to the articles [14, 34], as the author did for this thesis. A linear structural equation model given by a graph is a family of covariances parameterized by certain path structures within the graph. In Chapter 5, we are interested in understanding the parameters where the covariance parameterization fails to be generically locally injective for linear structural equation models given by acyclic mixed graphs. In this setting, the parameters where the covariance parameterization fails to be generically locally injective can be understood as the singularities of the covariance parameterization. Similar calculations are carried out in [17] under the setting of linear compartment models. The results in this thesis are preliminary results of on-going research and present the equations which define the singularities. Furthermore, we show that if the model is given by a union of disjoint paths, then the equations defining the singularities are monomial.

Before introducing the three models investigated in this thesis, we first introduce the language of algebraic geometry which is a tool that ties these models under one umbrella.

1.1 Ideals and Varieties

Let \mathbb{K} denote a (not necessarily algebraically closed) field. Usually \mathbb{K} denotes the field of rational numbers \mathbb{Q} , the field of real numbers \mathbb{R} , or the field of complex numbers \mathbb{C} . For symbolic computations \mathbb{K} is typically the former, while for theoretical reasons \mathbb{K} is usually the latter. Let \mathbb{Z} denote the set of integers and $\mathbb{Z}_{\geq 0}$ denote the set of non-negative integers. The role of algebraic geometry is to connect the algebra of polynomial rings to geometry. The main objects therefore live in the ring $\mathbb{K}[x_1, x_2, \dots, x_n]$ of polynomials in n indeterminates.

Definition 1.1. A *monomial* in the indeterminates x_1, x_2, \dots, x_n is a product $\mathbf{x}^{\mathbf{a}} := x_1^{a_1} x_2^{a_2} \cdots x_n^{a_n}$ for some $\mathbf{a} = (a_1, a_2, \dots, a_n) \in \mathbb{Z}_{\geq 0}^n$. A *polynomial* over \mathbb{K} in n indeterminates is a map $f : \mathbb{K}^n \rightarrow \mathbb{K}$ such that

$$f(\mathbf{x}) = \sum_{\mathbf{a} \in \mathcal{A}} c_{\mathbf{a}} \mathbf{x}^{\mathbf{a}}.$$

where $c_{\mathbf{a}} \in \mathbb{K}$ is a nonzero constant for all $\mathbf{a} \in \mathcal{A}$ and \mathcal{A} is a finite set called the *support* of f , also denoted as $\text{supp}(f)$.

Using multi-index notation, the ring $\mathbb{K}[x_1, x_2, \dots, x_n]$ will be abbreviated $\mathbb{K}[\mathbf{x}]$ where $\mathbf{x} = (x_1, x_2, \dots, x_n)$.

Definition 1.2. Let $f_1(\mathbf{x}), f_2(\mathbf{x}), \dots, f_m(\mathbf{x})$ be polynomials in $\mathbb{K}[\mathbf{x}]$. The *affine variety* defined by f_1, f_2, \dots, f_m is the set

$$V(f_1, f_2, \dots, f_m) = \{\mathbf{x} \in \mathbb{K}^n \mid f_i(\mathbf{x}) = 0 \text{ for all } 1 \leq i \leq m\}$$

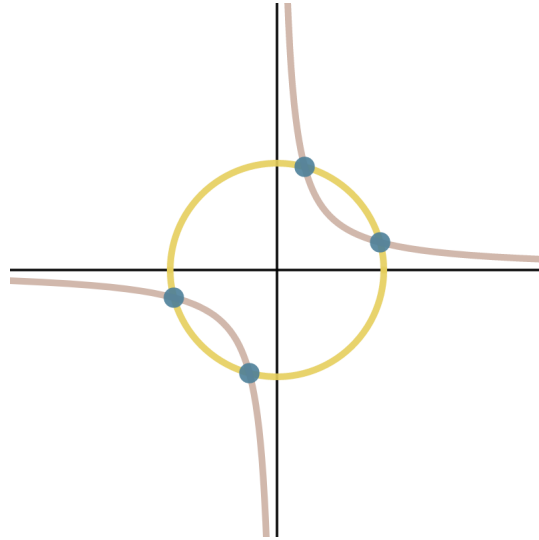


Figure 1.1: A variety shown as the four point intersection of two hypersurfaces, a circle and a hyperbola.

Example 1.3. Let $n = m = 2$. The variety defined by $f_1 = x^2 + y^2 - 4$ and $f_2 = xy - 1$ consists of the four points $(x, \frac{1}{x})$ where $x = \pm\sqrt{2 \pm \sqrt{3}}$. It is the intersection of a circle and a hyperbola, see Figure 1.1.

There are many more polynomials other than f_1, \dots, f_m that vanish at the points in the variety $V(f_1, \dots, f_m)$. In Example 1.3, the variety contained four points $(x, \frac{1}{x})$ with $x = \pm\sqrt{2 \pm \sqrt{3}}$. Consider for example the polynomial $h(x, y) = y^3 + x - 4y$. This polynomial will also vanish at the points $(x, \frac{1}{x})$, that is $h(x, \frac{1}{x}) = 0$. It is not a coincidence that $h = yf_1 + xf_2$. In general, any polynomial of the form $\sum_{i=1}^m g_i f_i$ for any choice of polynomials $g_i \in \mathbb{K}[\mathbf{x}]$ will vanish at all points in the variety $V(f_1, \dots, f_m)$. The set of all polynomials obtained as such is called an ideal.

Definition 1.4. Let $I \subseteq \mathbb{K}[\mathbf{x}]$. Then I is an *ideal* of $\mathbb{K}[\mathbf{x}]$ if

1. $0 \in I$

2. if $f, g \in I$, then $f + g \in I$
3. if $f \in I$ and $g \in \mathbb{K}[\mathbf{x}]$, then $gf \in I$.

Given polynomials f_1, \dots, f_m in $\mathbb{K}[\mathbf{x}]$, the *ideal generated by* f_1, \dots, f_m is the set

$$\langle f_1, \dots, f_m \rangle = \left\{ \sum_{i=1}^m h_i f_i \mid h_i \in \mathbb{K}[\mathbf{x}] \right\}.$$

As noted earlier, all polynomials in the ideal $I(f_1, \dots, f_m)$ vanish at all points in the variety defined by polynomials f_1, \dots, f_m . This justifies the following notation: given an ideal $I \subseteq \mathbb{K}[\mathbf{x}]$, define

$$V(I) = \{ \mathbf{x} \mid f(\mathbf{x}) = 0 \text{ for all } f \in I \}.$$

If I is generated by the polynomials f_1, \dots, f_m , then $V(I) = V(f_1, \dots, f_m)$. The following theorem states that every ideal is of this form, namely every ideal is finitely generated.

Theorem 1.5 (Hilbert's basis theorem). If \mathbb{K} is a Noetherian ring, then $\mathbb{K}[\mathbf{x}]$ is a Noetherian ring.

In other words, Hilbert's basis theorem says that given an ideal $I \subseteq \mathbb{K}[\mathbf{x}]$, there exists polynomials f_1, \dots, f_m such that $I = \langle f_1, \dots, f_m \rangle$.

Definition 1.6. Let I be an ideal of $\mathbb{K}[\mathbf{x}]$. The *radical* of I denoted \sqrt{I} is the set of all $f \in \mathbb{K}[\mathbf{x}]$ such that $f^k \in I$ for some positive integer k .

Example 1.7. Consider the ideal $I = \langle x^4 \rangle \subseteq \mathbb{K}[x]$ generated by x^4 . The radical of this ideal contains x since some powers of x belong to I , in particular x^4 . Thus, $\sqrt{I} = \langle x \rangle$.

Theorem 1.8 (Hilbert’s Nullstellensatz). Let I be an ideal of $\mathbb{K}[\mathbf{x}]$. If $f \in \mathbb{K}[\mathbf{x}]$ vanishes at all points in $V(I)$ i.e. $f(\mathbf{a}) = 0$ for all $\mathbf{a} \in V(I)$, then $f \in \sqrt{I}$.

We note that the converse of this statement is true, even though it is usually stated as above. Thus, Hilbert’s Nullstellensatz gives us a correspondence between ideals and varieties that we use often in applied algebraic geometry.

1.2 Polyhedral Geometry

There are many deep connections between algebraic geometry and polyhedral geometry. Here we introduce a few basic polyhedral objects that will play large roles in Chapter 3 and Chapter 4.

Definition 1.9. A *polytope* P is the convex hull of a finite set of points $\mathbf{p}_1, \dots, \mathbf{p}_m$ in \mathbb{R}^n , written

$$P = \text{conv}(\mathbf{p}_1, \dots, \mathbf{p}_m) = \left\{ \sum_{i=1}^m c_i \mathbf{p}_i \mid c_i \geq 0, \sum_{i=1}^m c_i = 1 \right\}$$

Example 1.10. The convex hull of the five points $(0, 0)$, $(0, .5)$, $(1, 0)$, $(0, 1)$, and $(1, 1)$ is a square, see Figure 1.2.

Definition 1.11. The *dimension* of a polytope $P \subset \mathbb{R}^n$ denoted $\dim P$ is the smallest nonnegative integer d such that P is contained in an affine subspace of \mathbb{R}^n of dimension d .

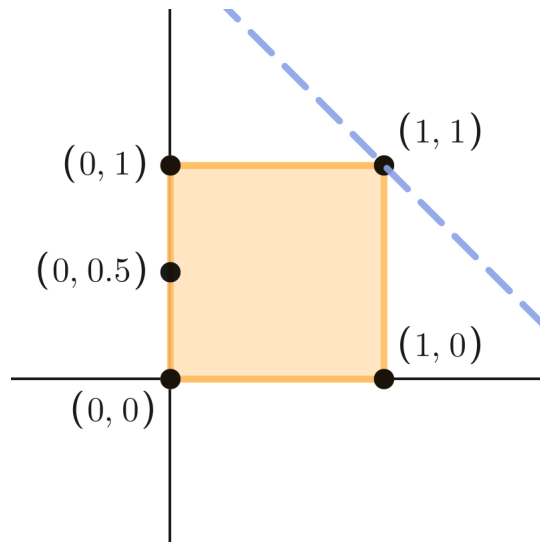


Figure 1.2: Illustration of the square polytope from Example 1.10.

Definition 1.9 alludes to what is known as a vertex representation, or v-representation, of P . In other words, it is a description of P by its vertices. Alternatively, polytopes can also be described by linear inequalities which bound the polytope. This description of P is called a half-space representation, or h-representation, of P .

Definition 1.12. A *hyperplane* in \mathbb{R}^n is the affine variety of the linear polynomial $\mathbf{a}\mathbf{x} - b$ where $\mathbf{a} \in \mathbb{R}^n$ and $b \in \mathbb{R}$. A hyperplane cuts \mathbb{R}^n into the two *half-spaces*: points \mathbf{x} satisfying $\mathbf{a}\mathbf{x} \geq b$ and $\mathbf{a}\mathbf{x} \leq b$. A *supporting hyperplane* of a polytope P is a hyperplane intersecting P such that P is contained entirely in one of its half-spaces.

Example 1.13. Let $P \subset \mathbb{R}^2$ be the square polytope in Figure 1.2. The (dashed blue) hyperplane $(1, 1)\mathbf{x} = x_1 + x_2 = 2$ is supporting since it intersects P at $(1, 1)$ and P is entirely contained in $x_1 + x_2 \leq 2$, i.e. every point

$\mathbf{p} \in P$ satisfies $p_1 + p_2 \leq 2$.

Definition 1.14. Let P be a polytope in \mathbb{R}^n . A *face* of P is the intersection of P with a supporting hyperplane.

Example 1.15. The square polytope in Figure 1.2 has four 0-dimensional faces $(0, 0)$, $(1, 0)$, $(0, 1)$, and $(1, 1)$. It has four 1-dimensional faces: line segments from $(0, 0)$ to $(1, 0)$, $(0, 0)$ to $(0, 1)$, $(1, 0)$ to $(1, 1)$, and $(0, 1)$ to $(1, 1)$.

A key polyhedral player for later chapters is a polytope obtained from smaller polytopes via an operation called a Minkowski sum. We end this polyhedral introduction with the definition of a Minkowski sum and produce an example of this operation on two polytopes in the plane.

Definition 1.16. Given a polytope $P \subset \mathbb{R}^n$ and a scalar $\lambda \in \mathbb{R}$, the dilate λP of P is the polytope

$$\lambda P = \{\lambda \mathbf{p} \mid \mathbf{p} \in P\}$$

where $\lambda \mathbf{p} = (\lambda p_1, \dots, \lambda p_n)$ is a coordinate-wise multiplication by λ .

Definition 1.17. Let P and Q be polytopes in \mathbb{R}^n . The *Minkowski sum* of P and Q is

$$P + Q = \{\mathbf{p} + \mathbf{q} \mid \mathbf{p} \in P, \mathbf{q} \in Q\}.$$

Example 1.18. Consider the polytopes $P = \text{conv}\{(1, 0), (0, 1), (0, -1), (-1, 0)\}$ and $Q = \text{conv}\{(0, 1), (1, 0), (0, 2), (1, 1), (2, 0)\}$. Their Minkowski sum $P + Q$ is the polytope $\text{conv}\{(0, 3), (3, 0), (2, -1), (1, -1), (-1, 2), (-1, 1)\}$. These three polytopes are drawn in Figure 1.3.

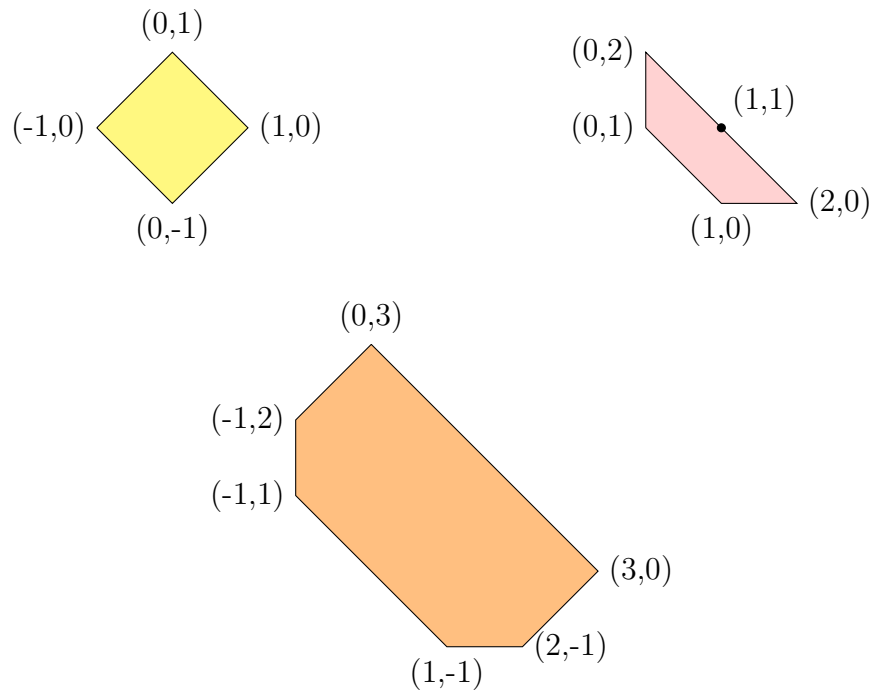


Figure 1.3: The cross polytope P (top left), a trapezoid Q (top right), and their Minkowski sum (bottom).

1.3 Zero-dimensional Solution Sets

Perhaps a best case scenario for mathematical models viewed as solution sets defined by polynomials or affine varieties is when these solution sets are “small” in the sense that their dimension is small. The first instance of such a small solution set is a zero-dimensional affine variety, i.e. a variety consisting of a finite number of points (a consequence of the fact that a variety can be written as a finite union of irreducible varieties [8]). For instance, the variety defined in Example 1.3 is zero-dimensional since it consists of four points.

Theorem 1.19 (Bézout’s Theorem). Let f_1, \dots, f_n be polynomials in $\mathbb{C}[\mathbf{x}]$

in n variables. Then either $f_1(\mathbf{x}) = \cdots = f_n(\mathbf{x}) = 0$ has infinitely many solutions or the number of solutions is at most $\prod_{i=1}^n \deg(f_i)$ counted with multiplicity.

Remark. For a more detailed description of multiplicity, as used above, please see appendix A in [18].

It can be very important to know the number of solutions of an affine variety for at least two reasons: to provide a measure on the algebraic complexity for solving $f(\mathbf{x}) = 0$ and for numerically computing solutions via polynomial homotopy continuation. For the former, this measure can give statistical information depending on the application. For example, concerning model selection, that is deciding whether or not a model is a good fit, algebraic complexity can be a criteria for model rejection if there is a prior expectation on the number of solutions.

A problem in using polynomial homotopy continuation (for specific details see [16, 35]), a method that tracks solutions from a start system to a given target system, is in finding an appropriate start system. In particular, an appropriate start system is one with the same number of solutions as the target system. For target systems with few polynomials and variables or polynomials with small degree, a *total degree* start system will suffice since Bézout's Theorem guarantees the number of solutions not to exceed $\prod_i \deg(f_i)$. However, for target systems consisting of polynomials with large degree, a total degree start system becomes computationally expensive.

Another option for a start system is to take advantage of the structure of the polynomials in the target system. Specifically, if the polynomials in the target system are sparse, i.e. polynomials with fewer terms than its degree

and number of variables suggest, then the number of solutions expected is typically far less than the total degree. In this case, an appropriate start system is called a *polyhedral* start system. The number of solutions of a polyhedral start system is equal to the volume of a polytope called a *mixed volume*. The following definition is also stated in [32] using the notation $[n] = \{1, 2, \dots, n\}$.

Definition 1.20. Let P_1, P_2, \dots, P_n be polytopes in \mathbb{R}^n . The *mixed volume* of polytopes P_1, P_2, \dots, P_n is

$$\text{MVol}(P_1, \dots, P_n) = \sum_{J \subset [n]} (-1)^{n-|J|} \cdot \text{volume} \left(\sum_{j \in J} P_j \right)$$

where **volume** denotes the usual Euclidean volume in \mathbb{R}^n .

Remark. Mixed volume can be defined more generally, where the number of polytopes does not equal the dimension of the ambient space [3]. However, since the goal is to apply this tool to square polynomials systems, these two numbers agree so we shall state this special version here instead.

A method for computing a mixed volume involves partitioning, or subdividing, the polytope into sections and computing volumes of smaller polytopes. The method described here is in terms of polytopes P_1, P_2, \dots, P_n in \mathbb{R}^n with $P_i = \text{conv}A_i$ but the same construction is also described in [21] viewing each P_i as the Newton polytope of some polynomial. Here $M = P_1 + \dots + P_n$ is their Minkowski sum.

Let C_i be a subpolytope of P_i , i.e. C_i is the convex hull of a nonempty subset of A_i . The Minkowski sum $C_1 + \dots + C_n$ is called a *cell* of M . A cell

$C = C_1 + \cdots + C_n$ is called *mixed* if $\dim C_i = 1$ for all $i = 1, \dots, n$. In other words, a mixed cell is a Minkowski sum of line segments.

Definition 1.21. A *subdivision* S of M is a set $\{C^{(1)}, \dots, C^{(k)}\}$ of cells of M such that

1. $\dim C^{(j)} = \dim M$ for all $j = 1, \dots, k$
2. $C^{(i)} \cap C^{(j)}$ is a face of both $C^{(i)}$ and $C^{(j)}$
3. $\bigcup_{j=1}^k C^{(j)} = M$

Further, the subdivision S is *mixed* if S satisfies the additional condition

4. $\sum_{i=1}^n \dim C_i^{(j)} = n$

for all $j = 1, \dots, k$.

Recall, a cell is a polytope so by $\dim C^{(j)}$ or $\dim C_i^{(j)}$ we mean its dimension as a polytope. Mixed subdivisions give a method for computing mixed volumes. The following statement gives a recipe for such a computation.

Theorem 1.22 ([21]). Let $S = \{C^{(1)}, \dots, C^{(k)}\}$ be a mixed subdivision of M . Then

$$\text{MVol}(P_1, \dots, P_n) = \sum_{\substack{C^{(j)} \in S \\ \text{mixed } C^{(j)}}} \text{vol}(C^{(j)}).$$

Example 1.23. A mixed subdivision of the Minkowski sum in Figure 1.3

consists of the seven cells

$$C^{(1)} = \text{conv}\{a, b\} + \text{conv}\{e, f\}$$

$$C^{(2)} = \text{conv}\{b, c\} + \text{conv}\{e, f\}$$

$$C^{(3)} = \text{conv}\{c\} + \text{conv}\{e, f, h, g\}$$

$$C^{(4)} = \text{conv}\{c, d\} + \text{conv}\{h, g\}$$

$$C^{(5)} = \text{conv}\{a, b, c, d\} + \text{conv}\{h\}$$

$$C^{(6)} = \text{conv}\{a, b\} + \text{conv}\{e, h\}.$$

We can see that the cells of this subdivision have dimension $\dim M = 2$, thus satisfying the first condition of a subdivision. The second and third conditions are easily seen in Figure 1.4.

This subdivision is indeed mixed since e.g. considering the cell $C^{(1)}$, we have $\dim \text{conv}\{a, b\} + \dim \text{conv}\{e, f\} = 2$. This mixed subdivision has four mixed cells: $C^{(1)}, C^{(2)}, C^{(4)}, C^{(6)}$. Thus by Theorem 1.22, the mixed volume of the Minkowski sum in Figure 1.3 is 5 since $\text{vol}(C^{(1)}) = \text{vol}(C^{(2)}) = \text{vol}(C^{(4)}) = 1$ and $\text{vol}(C^{(6)}) = 2$.

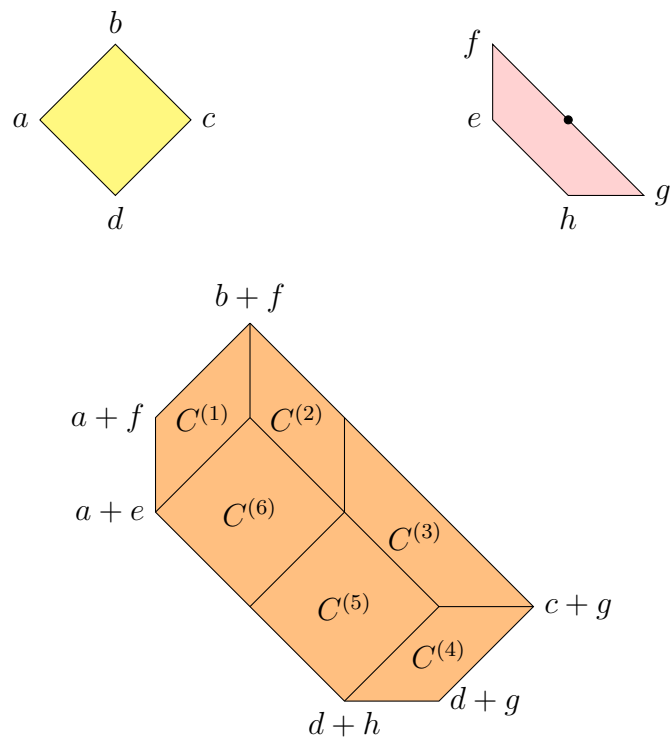


Figure 1.4: A mixed subdivision (bottom) of the cross polytope (top left) and a trapezoid (top left).

Chapter 2

Biological Models

This chapter contains a biological background of the three types of models where algebraic geometry plays the role.

2.1 Chemical Reaction Networks

Chemical reaction networks, sometimes called interaction networks, appear in many contexts ranging from analyzing the dynamical behavior of cellular signaling pathways in biochemistry to bifurcation analysis for disease control in epidemiology. Part of this thesis is concerned with chemical reaction networks under an assumption called *mass-action kinetics* (see Definition 2.1), an assumption that invites mathematicians to study the algebra and geometry arising from these network models. The reader can also refer to the article [19].

In the literature of chemical reaction network theory, the language of chemistry is typically used. In Figure 2.1, the letters A , B , and C are used

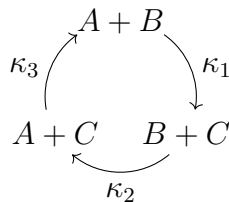


Figure 2.1: A cyclic chemical reaction network with three species and three reactions.

to denote what are called *species*. Depending on the context, the species can be chemical (e.g. molecules), biochemical (e.g. proteins, enzymes), humans in particular states (e.g. sick individuals, healthy individuals), and much more. The interactions of the species are encoded as formal sums of the letters with nonnegative integer coefficients. These formal sums are called *complexes*. For instance, the complex $A+B$ denotes an interaction between a single molecule of A and a single molecule of B . When species come together we expect that the interaction causes a change in the state of the species. These changes are represented via the arrows of the diagram. For instance, the arrow $A+B \rightarrow B+C$ should be interpreted as: when a single molecule of A interacts, or reacts, with a single molecule of B , the result is a production of a single molecule of B and a single molecule of C . In other words, if this reaction fires once we lose a molecule of A and gain a molecule of C while B remains unchanged. Further, it can also be said the species B acts as a catalyst, reacting with A to produce C .

The interest is in the evolution of the amount, or concentration, of the species over time. Given a diagram, or directed graph, as in Figure 2.1, a *reaction kinetics* of the directed graph is an assumption on precisely how the concentrations change over time. Formally, a reaction kinetics is a family of

propensity functions $v_i(\mathbf{x})$ called *reaction rates* that characterizes how often each reaction fires where $\mathbf{x} = (x_A, x_B, x_C)$ is a vector of concentrations of A, B and C . The most common type of reaction kinetics is called *mass-action kinetics*.

Definition 2.1. The law of *mass-action* states that the propensity of a reaction is proportional to the product of concentrations of reacting species, i.e. the reaction rate of the i th reaction $a_1X_1 + \dots + a_nX_n \rightarrow b_1X_1 + \dots + b_nX_n$ is

$$v_i(\mathbf{x}) = \kappa_i x_1^{a_1} \dots x_n^{a_n}$$

where κ_i is a positive real number called a *reaction rate constant*.

For instance, it is expected the reaction rate of the reaction $A+B \rightarrow B+C$ to be $v_1(\mathbf{x}) = \kappa_1 x_A x_B$. The positive real number κ_1 is a proportionality constant – it can be thought to govern the “speed” of the first reaction. The reaction rate constants are encoded into the directed graph as edge weights of the corresponding edge. Lastly, the sign on the term $-\kappa_1 x_A x_B$ reflects a loss of one molecule of A in this reaction.

Therefore, mass-action kinetics gives rise to the parameterized polynomial ordinary differential equations:

$$\frac{d}{dt} \begin{pmatrix} x_A \\ x_B \\ x_C \end{pmatrix} = \begin{pmatrix} -\kappa_1 x_A x_B + \kappa_2 x_B x_C \\ -\kappa_2 x_B x_C + \kappa_3 x_A x_C \\ \kappa_1 x_A x_B - \kappa_3 x_A x_C \end{pmatrix}.$$

In this thesis, a chemical reaction network will be thought of as a directed graph without self-loops or isolated vertices as in the definition below. In

this definition, the complexes of the network are identified with points in $\mathbb{Z}_{\geq 0}^n$, e.g. the complex $A + B$ will be thought of as the vector of coefficients $(1, 1, 0)^T$ in $\mathbb{Z}_{\geq 0}^3$.

Definition 2.2. A *chemical reaction network* on n species is a directed graph $G = (\mathcal{C}, \mathcal{R})$ where $\mathcal{C} \subset \mathbb{Z}_{\geq 0}^n$ is a finite subset, the set of complexes. The edge set, or set of reactions, \mathcal{R} is a relation \rightarrow on \mathcal{C} such that $\mathbf{y} \rightarrow \mathbf{y} \notin \mathcal{R}$ for any $\mathbf{y} \in \mathcal{C}$.

For each reaction $\mathbf{y}_i \rightarrow \mathbf{y}_j$ of the network, the vector $\mathbf{y}_j - \mathbf{y}_i$ will be called a *reaction vector*. Its entries encode the net change of production for each species in the corresponding reaction. The matrix N whose columns consist of all reaction vectors is called the *stoichiometric matrix*. The matrix B whose columns are \mathbf{y}_i whenever $\mathbf{y}_i \rightarrow \mathbf{y}_j$ is a reaction is called the *reactant matrix*. Example 2.4 gives the stoichiometric matrix and reactant matrix corresponding to the chemical reaction network of Figure 2.1.

Using multi-index notation, let \mathbf{x} denote the vector of concentrations $(x_1, x_2, \dots, x_n)^T$. If $\mathbf{y} \in \mathbb{Z}_{\geq 0}^n$, then $\mathbf{x}^{\mathbf{y}}$ denotes the monomial $x_1^{y_1} x_2^{y_2} \dots x_n^{y_n}$. If B is a matrix with n rows and integer entries, then \mathbf{x}^B denotes a vector of monomials corresponding to the columns of B , i.e. if \mathbf{b}_i is the i -th column of B , then $\mathbf{x}^{\mathbf{b}_i}$ is the i -th entry of \mathbf{x}^B .

Definition 2.3. Given a chemical reaction network G together with a choice of reaction rate constants $\boldsymbol{\kappa} \in \mathbb{R}_{> 0}^n$, the polynomial ODE system

$$\frac{d\mathbf{x}}{dt} = f(\mathbf{x}, \boldsymbol{\kappa}) := N \text{diag}(\boldsymbol{\kappa}) \mathbf{x}^B \quad (2.1)$$

is called the *mass-action system* where N is the stoichiometric matrix, $\text{diag}(\boldsymbol{\kappa})$

is a diagonal matrix with κ_i on its diagonal, and B is the reactant matrix. The ideal generated by the equations $f_1(\mathbf{x}, \boldsymbol{\kappa}), \dots, f_n(\mathbf{x}, \boldsymbol{\kappa})$ is called the *mass-action ideal*.

Example 2.4. The mass-action system associated to the chemical reaction network of Figure 2.1 has matrices

$$N = \begin{pmatrix} -1 & 1 & 0 \\ 0 & -1 & 1 \\ 1 & 0 & -1 \end{pmatrix}, \quad B = \begin{pmatrix} 1 & 0 & 1 \\ 1 & 1 & 0 \\ 0 & 1 & 1 \end{pmatrix},$$

$$\text{diag}(\boldsymbol{\kappa}) = \begin{pmatrix} \kappa_1 & 0 & 0 \\ 0 & \kappa_2 & 0 \\ 0 & 0 & \kappa_3 \end{pmatrix}, \quad \text{and} \quad \mathbf{x}^B = \begin{pmatrix} x_A x_B \\ x_B x_C \\ x_A x_C \end{pmatrix}.$$

Depending on the network, the ordinary differential equation $\frac{d\mathbf{x}}{dt} = f_{\boldsymbol{\kappa}}(\mathbf{x})$ can satisfy trivial solutions that arise from $\ker N^T$. Let $d = \dim \ker N^T$. If W is a $d \times n$ matrix such that $WN = 0$ then $Wf(\mathbf{x}) = 0$. By integrating this equation we get the linear equation $W\mathbf{x} = \mathbf{c}$ where $\mathbf{c} \in \mathbb{R}^d$ is determined by the initial concentrations $\mathbf{x}(0)$ at the start of the system. In other words, the system $\frac{d\mathbf{x}}{dt} = f(\mathbf{x})$ can have linear relationships among the equations and each give rise to linear relationships among the variables. If \mathbf{w} is the i -th row of W , the linear equation $\mathbf{w} \cdot \mathbf{x} = c_i$ is called a *conservation law* as defined in [25]. We will refer to a row \mathbf{w} of W as a *conservation law vector* and the linear span of the conservation law vectors as the *space of conservation laws*.

For the purpose of having a square system, replace the redundant equations according to the procedure as in [27]: suppose W is a row reduced

matrix such that $WN = 0$. For each row vector \mathbf{w}_i of W , let $j(i)$ be the index of the first nonzero entry of \mathbf{w}_i . Then replace $f_{j(i)}(\mathbf{x})$ with the linear polynomial $\mathbf{w}_i \cdot \mathbf{x} - c_i$. If J is the set of all $j(i)$ for all $i = 1, \dots, d$, the new set of equations can then be written as

$$f(\mathbf{x}) := f(\mathbf{x}, \boldsymbol{\kappa}, \mathbf{c}) = \begin{cases} f_i(\mathbf{x}, \boldsymbol{\kappa}) & \text{if } i \notin J \\ \mathbf{w}_i \cdot \mathbf{x} - c_i & \text{if } i = j(i) \in J \end{cases} \quad (2.2)$$

Definition 2.5. Given a chemical reaction network G , reaction rate constants $\boldsymbol{\kappa} \in \mathbb{R}^n$, and total concentration vector $\mathbf{c} \in \mathbb{R}^d$, the polynomial system in (2.2) is called the *steady-state system*. The ideal generated by the equations f_1, \dots, f_n is called the *steady-state ideal*.

Example 2.6. Let G be the cycle network as in Figure 2.1. The stoichiometric matrix associated with G is given in Example 2.4. The left kernel of this matrix is spanned by the conservation law vector $\mathbf{w} = (1, 1, 1)$. Since the first entry of this vector is nonzero, then the steady-state system of G is the mass-action system of G with its first equation replaced by the linear polynomial $(1, 1, 1) \cdot \mathbf{x} - c_1$. Thus the steady-state system of G is

$$f(\mathbf{x}) = \begin{cases} x_A + x_B + x_C - c_1 \\ -\kappa_2 x_B x_C + \kappa_3 x_A x_C \\ \kappa_1 x_A x_B - \kappa_3 x_A x_C \end{cases}$$

for some choice of positive real parameters $\kappa_1, \kappa_2, \kappa_3$, and c_1 .

Definition 2.7. A *steady-state* of $\frac{d\mathbf{x}}{dt} = f(\mathbf{x})$ is a point $\mathbf{x} \in \mathbb{R}^n$ such that $f(\mathbf{x}) = 0$. The *steady-state variety* is the set of all steady-states of $\frac{d\mathbf{x}}{dt} = f(\mathbf{x})$,

that is the variety defined by the polynomials f_1, \dots, f_n . The *steady-state degree* of a chemical reaction network is the number of nonzero complex points in the steady-state variety for generic reaction rate constants and initial concentrations.

Example 2.8. Using the computer algebra software `Macaulay2`, we can numerically approximate the steady-state variety given by the system in Example 2.6 for the (randomly generated) parameters $c_1 = \frac{41}{9}$, $\kappa_1 = 10$, $\kappa_2 = -\frac{9}{2}$, and $\kappa_3 = \frac{6}{7}$. It consists of the four points

$$\{(4.56, 0, 0), (0, 4.56, 0), (0, 0, 4.56), (1.33, .25, 2.97)\} \subset \mathbb{R}^3$$

so we expect the steady-state degree to be one.

Remark. In the setting of chemical reaction networks, the true interest is in positive steady-states, i.e. steady-states with positive coordinates. However, the theory of semi-algebraic sets is far less strong than the theory of algebraic varieties. Regardless, in this thesis we shall remain interested in the nonzero complex steady-states, even if they are not positive or real, since our focus is on the algebra and combinatorics of chemical reaction networks.

2.2 Phylogenetic Trees

A phylogenetic tree is a graphical representation of the evolutionary history between a set of species or *taxa*. In this section, we introduce a mathematical framework for the biologically inspired phylogenetic tree reconstruction problem. Specifically, the interest is in compiling evolutionary relationships



Figure 2.2: Two phylogenetic tree on four taxa A , B , C , and D .

given a set of phylogenetic trees into a single phylogenetic tree. Here the approach is through tropical algebraic geometry and view the space of phylogenetic trees with a fixed number of leaves as a tropical linear subspace of $\mathbb{R}^{\binom{m}{2}}/\mathbb{R}\mathbf{1}$. We end this section with an example given two phylogenetic trees and introduce the tropical combinatorics that aids us along the way.

Definition 2.9. A (rooted) *phylogenetic tree* is an edge-weighted directed graph T having exactly one source vertex and its underlying graph has no cycles. The source vertex is called the *root* of the tree while a sink vertex is called a *leaf*.

Example 2.10. Consider a set of four taxa A , B , C , and D . Two possible graphical representations of their evolutionary relationships are depicted below. For both of these phylogenetic trees, the topology of the tree tells us e.g. A and B are more closely related than A and C . Said differently, the path from A to B is shorter than the path from A to C .

A description of how phylogenetic trees are parameterized is given in [24], especially how the tropical grassmanian is a moduli space for the space of phylogenetic trees. The following description is motivation for viewing the set of phylogenetic trees as a subset of $\mathbb{R}^{\binom{m}{2}}/\mathbb{R}\mathbf{1}$.

A phylogenetic tree has a unique path between any pair of its leaf vertices. Define the distance v_{ij} between a pair of distinct leaves to be the sum of the edge weights along the path between them. The vector $\mathbf{v} = (v_{ij})$ arising from a phylogenetic tree is called a *tree metric*. Allowing the edge weights of the tree to be any real number, the resulting space of tree metrics is not a metric space. However, adding large multiples of $\mathbb{1} = (1, 1, \dots, 1)$ will yield an honest tree metric. Thus, the set of tree metrics will be viewed as a subset of $\mathbb{R}^{\binom{m}{2}}/\mathbb{R}\mathbb{1}$.

A main problem in phylogenetics is to use current data, maybe DNA from living species, to reconstruct their true evolutionary relationships represented by a phylogenetic tree. Often there are errors in the resulting phylogenetic tree but if it can be somehow proven the phylogenetic tree represents the true evolutionary relationships, the tree is called the *true phylogeny*. Besides errors in phylogenetic tree reconstruction, another issue in this setting is that there are several methods for reconstructing phylogenetic trees and the various resulting trees typically do not agree. Thus, a key hurdle is to overcome the choice of tree which best represents the true evolutionary data. A common strategy is to gather information from many trees and compile this information into a single tree. The resulting tree obtained from such a strategy is called a *consensus tree*. Still there are many consensus methods for computing a consensus tree. For a survey of consensus methods see [2]. While many consensus methods rely on the topology of the trees, our the approach is through tropical geometry.

In this thesis, the phylogenetic trees considered are called *equidistant*, i.e. the distance from the root to leaf is the same for all leaves of the tree.

Let $\Delta \subset \mathbb{R}^{\binom{m}{2}}/\mathbb{R}\mathbb{1}$ be the set of equidistant phylogenetic trees and d be a metric on Δ . The consensus tree question can be stated as an optimization problem. Given tree metric $\mathbf{v}_1, \dots, \mathbf{v}_k \in \Delta$, find a tree metric \mathbf{v} that minimizes the distances $d(\mathbf{v}, \mathbf{v}_i)$, or equivalently minimizes the sum of distances $\sum_{i=1}^k d(\mathbf{v}, \mathbf{v}_i)$. Geometrically, this is a problem of finding the median of a data set. These types of problems are also known as *Fermat-Weber problems*. In this more general setting, points \mathbf{v} which minimize the above sum are called *Fermat-Weber points*. While the focus is on finding consensus trees, we shall adopt the Fermat-Weber language to remain suggestive of this more general problem.

In [5], the authors solve the consensus tree problem with the asymmetric metric (Equation 4.6) on Δ . They take advantage of polyhedral geometry and linear optimization to locate Fermat-Weber points. In this thesis, the interest is in generalizing this result by slightly modifying the question: given tree metrics $\mathbf{v}_1, \dots, \mathbf{v}_k$ and positive weights w_i , find the points \mathbf{v} which minimize the weighted sum $\sum_{i=1}^k w_i d(\mathbf{v}, \mathbf{v}_i)$. The remainder of this section introduces a mathematical framework where this *weighted Fermat-Weber problem* can be solved.

A *polyhedral complex* is a collection of polyhedra $S = \{C_i\}$ with the following properties: (1) S is closed under taking faces, and (2) $C_i \cap C_j$ is a face of both C_i and C_j , or is empty. The *normal cone to F in P* , denoted σ_F , is the set of all vectors $u \in (\mathbb{R}^m)^*$ such that $\text{face}_{\mathbf{u}}(P) \supseteq F$ where

$$\text{face}_{\mathbf{u}}(P) := \{\mathbf{x} \in P \mid \mathbf{u} \cdot \mathbf{x} \leq \mathbf{u} \cdot \mathbf{y}, \forall \mathbf{y} \in P\}.$$

Alternatively, σ_F is the closure of $\{\mathbf{u} \in (\mathbb{R}^m)^* \mid \text{face}_{\mathbf{u}}(P) = F\}$. The *normal fan* of a polytope P is the collection of cones $\{\sigma_F \mid F \text{ a face of } P\}$.

For the remainder of this section we are concerned with subdivisions of polytopes. Consider m polytopes $P_1, \dots, P_m \subset \mathbb{R}^n$ where $P_i = \text{conv}(A_i)$ for some finite sets $A_i \subset \mathbb{R}^n$.

Definition 2.11. Given a polytope $P = \text{conv}\{\mathbf{v}_1, \dots, \mathbf{v}_k\} \subset \mathbb{R}^n$, and weights $w_i \in \mathbb{R}$ on \mathbf{v}_i , the *lift* of P with respect to \mathbf{w} is

$$\tilde{P} := \text{conv}\{(\mathbf{v}_i, w_i) \mid i = 1, \dots, k\} \subset \mathbb{R}^{n+1} \quad (2.3)$$

A face $F = \text{face}_{\mathbf{u}}(\tilde{P})$ of \tilde{P} is an *upper face* if $u_{n+1} < 0$. The *regular subdivision of P with respect to \mathbf{w}* is the projection of the upper faces of \tilde{P} onto P (forgetting the last coordinate). An example is given in 4.12.

Definition 2.12. The *normal complex* of a regular subdivision is the projection of the cones of the normal fan of \tilde{P} that are normal to upper faces of \tilde{P} .

Notation: A subdivision of P will be denoted \underline{P} . Regular subdivisions induced by a piecewise linear convex function λ will be denoted \underline{P}_λ .

Definition 2.13. Let P_1, \dots, P_m be polytopes in \mathbb{R}^n . The Cayley polytope, $\text{Cayley}(P_1, \dots, P_m)$, is the convex hull of $\bigcup_{i=1}^m e_i \times P_i$ in $\mathbb{R}^m \times \mathbb{R}^n$. In the special case where $P_1 = P_2 = \dots = P_m$, the Cayley polytope is $\Delta^{r-1} \times P$. For an example see 4.3.

The Cayley trick is a correspondence between mixed subdivisions of the Minkowski sum $P_1 + \dots + P_m$ and subdivisions of $\text{Cayley}(P_1, \dots, P_m)$, illustrated in 4.3. The top right polytope in 4.3 is $\text{Cayley}(\Delta^2, \Delta^2) \cong \Delta^1 \times \Delta^2$.

Explicitly, a subdivision of the Cayley polytope gives rise to a subdivision of the Minkowski sum after forgetting the first m coordinates. For more details, see [31, Section 5] for coherent/regular subdivisions, and [20, Theorem 3.1] for all subdivisions.

We will refer to Definition 1.21 above as the *combinatorial Cayley trick*. In addition to the combinatorial correspondence above, there is also an explicit geometric correspondence between a subdivision of the Cayley polytope and a mixed subdivision, sometimes called the *geometric Cayley trick*.

Theorem 2.14 ([20, Theorem 3.1]). Let \underline{C} be a subdivision of $\text{Cayley}(P_1, \dots, P_m)$. Then the corresponding mixed subdivision of $P = \sum_{i=1}^m P_i$ is $\underline{P} = n \cdot \underline{C} \cap \{\frac{1}{m} \mathbb{1}_m\} \times \mathbb{R}^n$.

2.15 is essentially stated in [30, §1.3]. It allows us to think about mixed subdivisions of a *weighted* Minkowski sum, $P^{\mathbf{w}} = \sum_{i=1}^m w_i P_i$, in terms of the Cayley polytope without weights, $\text{Cayley}(P_1, \dots, P_m)$, by slicing at $\{\mathbf{w}\} \times \mathbb{R}^n$. We provide a proof that explicitly states the map that induces the bijection, which we will use later in the paper.

Proposition 2.15. Let $C = \text{Cayley}(P_1, \dots, P_m)$, and let $D = \text{cone}(C)$ denote the cone over it. Let $C^{\mathbf{w}}$, $D^{\mathbf{w}}$, and $P^{\mathbf{w}}$ denote the corresponding weighted versions, for $\mathbf{w} \in \mathbb{R}^m$ with $|\mathbf{w}| = 1$. Let λ be a piecewise linear convex function on $\text{Cayley}(w_1 P_1, \dots, w_m P_m)$, and let $g(\mathbf{x}, \mathbf{y}) = (w_1 x_1, \dots, w_m x_m, \mathbf{y})$.

If $\lambda' = \lambda(g^{-1}(x, y))$, then the following diagram commutes.

$$\begin{array}{ccc}
 \underline{D}_\lambda^{\mathbf{w}} & \xrightarrow{g} & \underline{D}_{\lambda'} \\
 \uparrow & & \uparrow \cap \{\sum_{i=1}^m x_i=1\} \\
 \underline{C}_\lambda^{\mathbf{w}} & \dashrightarrow & \underline{C}_{\lambda'} \\
 \swarrow \cap \left(\left\{\frac{1}{m}\right\} \times \mathbb{R}^n\right) \cap \bullet & & \searrow \bullet \cap (\{\mathbf{w}\} \times \mathbb{R}^n) \\
 & \underline{P}_\lambda^{\mathbf{w}} &
 \end{array}$$

Proof. The subdivision $\underline{C}_\lambda^{\mathbf{w}}$ induces a subdivision $\underline{D}_\lambda^{\mathbf{w}}$. The function g is an invertible linear function. In particular, this means g preserves convexity, dimension, and the containment relations within a polyhedral subdivision. Thus, $\underline{D}_\lambda^{\mathbf{w}}$ induces a subdivision $\underline{D}_{\lambda'}$ via $\lambda'(z) = \lambda(g^{-1}(z))$. This in turn induces a subdivision $\underline{C}_{\lambda'}$ with the weightings $\lambda'(e_i, v_{ij}) = \lambda(e_i, w_i v_{ij})$, which is combinatorially equivalent to $\underline{C}_\lambda^{\mathbf{w}}$. Moreover, $n \cdot \underline{C}_\lambda^{\mathbf{w}} \cap \left(\left\{\frac{1}{m}\right\} \times \mathbb{R}^n\right)$, and $\underline{C}_{\lambda'} \cap (\{\mathbf{w}\} \times \mathbb{R}^n)$ give the same subdivision of $\underline{P}_\lambda^{\mathbf{w}}$. \square

2.3 Linear Structural Equation Models

Structural equation models are a way to mathematically represent cause-effect hypotheses. These relationships are encoded into a graph and give rise to a system of equations. The causes and effects X_i are thought of as the vertices $i \in [n] = \{1, \dots, n\}$ of the graph and a directed edge (i, j) represents the hypothesis “ X_i causes the effect X_j ”.

If the relationships are assumed to be linear among the variables, then the resulting model is called a linear structural equation model. In this thesis, all structural equation models are assumed to be linear. The graphs that

give rise to the linear structural equation models are called mixed graphs. After defining a mixed graph, we formalize how a mixed graph gives rise to the model.

Definition 2.16. A *mixed graph* with vertex set V is a tuple (V, D, B) where $D, B \subseteq V \times V$ are two edge sets. The set D consists of ordered pairs (i, j) also denoted $i \rightarrow j$. The set B consists of unordered pairs $\{i, j\}$ also denoted $i \leftrightarrow j$.

A mixed graph $G = (V, D, B)$ is called *acyclic* if the direct part of the graph has no directed cycles, i.e. there does not exist a sequence of edges $i_0 \rightarrow i_1 \rightarrow \dots \rightarrow i_k \rightarrow i_0$ belonging to D . A directed path in G from i to j will be denoted as $i \rightarrow j$. The vertex i is called the *source* of the path $i \rightarrow j$ while j is called the *sink*. A source and sink are also denoted $\text{source}(i \rightarrow j)$ and $\text{sink}(i \rightarrow j)$, respectively. In this thesis, the directed part of a mixed graph is assumed to be topologically sorted, meaning $i \rightarrow j \in D$ only if $i < j$. A vertex i is called a *parent* of a vertex j if $i \rightarrow j \in D$. The set of all parents of a vertex j is denoted $\text{pa}(j)$. A vertex i is called an *ancestor* of j if there is a directed path from i to j . The set of all ancestors of a vertex j is denoted $\text{an}(j)$.

Example 2.17. Consider the mixed graph of Figure 2.3. It depicts a mixed graph on the vertex set $V = [4] = \{1, 2, 3, 4\}$. Its directed edges are $(1, 2)$ and $(1, 3)$ while its only bidirected edge is $\{1, 4\}$.

Let $G = (V, D, B)$ be a mixed graph with $V = [n]$. The graph G encodes a system of polynomial equations in $\mathbb{R}[X_1, \dots, X_n]$ where each vertex i of G is associated to the variable X_i . Directed paths in G represent dependencies

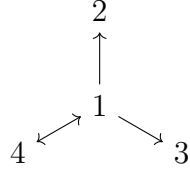


Figure 2.3: A star graph on four vertices with two directed edges and a single bidirected edge.

in the variables X_i . For instance, if G is the mixed graph in Figure 2.3, the directed edge $(1, 2)$ means X_2 is dependent on X_1 . In general, a directed edge (i, j) in G encodes a monomial term $\lambda_{ij}X_i$ where λ_{ij} is a real parameter measuring the strength of the dependence of X_j on X_i . The mixed graph in Figure 2.3 gives rise to the following linear equations.

$$\begin{aligned} X_1 &= && + \epsilon_1 \\ X_2 &= \lambda_{12}X_1 + \epsilon_2 \\ X_3 &= \lambda_{13}X_1 + \epsilon_3 \\ X_4 &= && + \epsilon_4 \end{aligned}$$

where ϵ_i are error terms according to a given normal distribution with mean zero. A bidirected edge $\{i, j\}$ in G encodes a dependence in error terms ϵ_i and ϵ_j . The above system of linear equations can be concisely written as the linear system

$$X = \Lambda^T X + \epsilon$$

where $X = (X_1, \dots, X_n)$ is a random variable of a multivariate normal distribution with mean zero, $\epsilon = (\epsilon_1, \dots, \epsilon_n)$, and Λ is an $n \times n$ matrix which has nonzero entries $\lambda_{ij} \in \mathbb{R}$ if (i, j) is a directed edge. This system has a

unique solution $X = (I - \Lambda)^{-T} \boldsymbol{\epsilon}$ and its covariance matrix is

$$\Sigma = (I - \Lambda)^{-t} \Omega (I - \Lambda)^{-1}$$

where I is the $n \times n$ identity matrix and Ω is a positive definite $n \times n$ matrix having nonzero entries ω_{ii} if i is a vertex and ω_{ij} if $\{i, j\}$ is a bidirected edge. Let $\mathbb{R}_{\text{reg}}^D$ be the set of all Λ such that $I - \Lambda$ is invertible. Let $PD(B)$ be the set of all positive definite matrices Ω having nonzero entries diagonal entries and whenever $\{i, j\}$ is a bidirected edge.

Definition 2.18. A *linear structural equation model* given by a mixed graph $G = (V, D, B)$ is

$$\mathcal{M}_G = \{(I - \Lambda)^{-t} \Omega (I - \Lambda)^{-1} \mid \Lambda \in \mathbb{R}_{\text{reg}}^D, \Omega \in PD(B)\}.$$

The *covariance parameterization* of the model is the map

$$\phi_G : \mathbb{R}^D \times PD(B) \rightarrow PD(V), \quad (\Lambda, \Omega) \mapsto (I - \Lambda)^{-t} \Omega (I - \Lambda)^{-1}$$

and define the *fiber* of $(\Lambda, \Omega) \in \mathbb{R}_{\text{reg}}^D \times PD(B)$ to be the preimage

$$\mathcal{F}(\Lambda, \Omega) = \{(\Lambda', \Omega') \in \mathbb{R}_{\text{reg}}^D \times PD(B) \mid \phi_G(\Lambda', \Omega') = \phi_G(\Lambda, \Omega)\}.$$

Example 2.19. The matrices associated with the linear structural equation

model given by the mixed graph of Figure 2.3 are

$$\Lambda = \begin{pmatrix} 0 & \lambda_{12} & \lambda_{13} & 0 \\ 0 & 0 & 0 & 0 \\ 0 & 0 & 0 & 0 \\ 0 & 0 & 0 & 0 \end{pmatrix} \quad \text{and} \quad \Omega = \begin{pmatrix} \omega_{11} & 0 & 0 & \omega_{14} \\ 0 & \omega_{22} & 0 & 0 \\ 0 & 0 & \omega_{33} & 0 \\ \omega_{14} & 0 & 0 & \omega_{44} \end{pmatrix}$$

and the covariance parameterization of the model is

$$\Sigma = \begin{pmatrix} \omega_{11} & \omega_{11}\lambda_{12} & \omega_{11}\lambda_{13} & \omega_{14} \\ \omega_{11}\lambda_{12} & \omega_{11}\lambda_{12}^2 + \omega_{22} & \omega_{11}\lambda_{12}\lambda_{13} & \omega_{14}\lambda_{12} \\ \omega_{11}\lambda_{13} & \omega_{11}\lambda_{12}\lambda_{13} & \omega_{11}\lambda_{13}^2 + \omega_{33} & \omega_{14}\lambda_{13} \\ \omega_{14} & \omega_{14}\lambda_{12} & \omega_{14}\lambda_{13} & \omega_{44} \end{pmatrix}.$$

The entries of the covariance parameterization of the model can be combinatorially realized from certain paths in the mixed graph.

Definition 2.20. Let $G = (V, D, B)$ be a mixed graph. A *trek* from i to j is a pair of directed paths $(i_0 \rightarrow i, j_0 \rightarrow j)$ such that either $i_0 = j_0$ or $i_0 \leftrightarrow j_0$ is a bidirected edge in B , i.e. a trek is one of two forms

1. $i \leftarrow i_k \leftarrow \cdots \leftarrow i_0 \rightarrow \cdots \rightarrow j_\ell \rightarrow j$, or
2. $i \leftarrow i_k \leftarrow \cdots \leftarrow i_0 \leftrightarrow j_0 \rightarrow \cdots \rightarrow j_\ell \rightarrow j$.

In either case, the bidirected edge $i_0 \leftrightarrow j_0$ or the vertex i_0 is called the *peak* of the trek.

Let $\mathcal{T}(i, j)$ be the set of all treks from i to j . Expanding the product

$(I - \Lambda)^{-t} \Omega (I - \Lambda)^{-1}$ gives the *trek rule* for the covariance matrix $\Sigma = (\sigma_{ij})$:

$$\sigma_{ij} = \sum_{(P, P') \in \mathcal{T}(i, j)} \text{peak}(P, P') \lambda^P \lambda^{P'} \quad (2.4)$$

where

$$\lambda^P = \prod_{(k, \ell) \in P} \lambda_{k\ell}$$

and

$$\text{peak}(P, P') = \begin{cases} \omega_{i_0 i_0} & \text{if } \text{source}(P) = \text{source}(P') \\ \omega_{i_0 j_0} & \text{if } \text{source}(P) \leftrightarrow \text{source}(P') \in B. \end{cases}$$

By convention, if P is a directed path with no edges then $\lambda^P = 1$. This thesis is concerned with the ability to recover the parameters λ_{ij} .

Definition 2.21. Let G be a mixed graph. The map ϕ_G is

1. *injective* if the fiber $\mathcal{F}(\Lambda, \Omega) = \{(\Lambda, \Omega)\}$ is a singleton for all choices $(\Lambda, \Omega) \in \mathbb{R}_{\text{reg}}^D \times PD(B)$.
2. *generically injective* if the fiber $\mathcal{F}(\Lambda, \Omega) = \{(\Lambda, \Omega)\}$ is a singleton for generic choices of $(\Lambda, \Omega) \in \mathbb{R}_{\text{reg}}^D \times PD(B)$.
3. *generically locally identifiable* if the fiber $\mathcal{F}(\Lambda, \Omega)$ is finite for generic choices of $(\Lambda, \Omega) \in \mathbb{R}_{\text{reg}}^D \times PD(B)$.

Deciding whether the covariance parameterization ϕ_G is generically locally identifiable is equivalent to the Jacobian of ϕ_G generically having full column rank. This is also equivalent to the existence of some $d \times d$ minor of the Jacobian generically not vanishing where $d = |V| + |D| + |B|$, or in the

language of algebraic geometry the ideal of minors is nonzero for generic parameters.

Example 2.22. The Jacobian of the covariance parameterization ϕ_G where G is the mixed graph in Figure 2.3 is

$$\begin{pmatrix} 1 & 0 & 0 & 0 & 0 & 0 & 0 \\ \lambda_{12} & 0 & 0 & 0 & 0 & \omega_{11} & 0 \\ \lambda_{13} & 0 & 0 & 0 & 0 & 0 & \omega_{11} \\ 0 & 0 & 0 & 0 & 1 & 0 & 0 \\ \lambda_{12}^2 & 1 & 0 & 0 & 0 & 2\omega_{11}\lambda_{12} & 0 \\ \lambda_{12}\lambda_{13} & 0 & 0 & 0 & 0 & \omega_{11}\lambda_{13} & \omega_{11}\lambda_{12} \\ 0 & 0 & 0 & 0 & \lambda_{12} & \omega_{14} & 0 \\ \lambda_{13}^2 & 0 & 1 & 0 & 0 & 0 & 2\omega_{11}\lambda_{13} \\ 0 & 0 & 0 & 0 & \lambda_{13} & 0 & \omega_{14} \\ 0 & 0 & 0 & 1 & 0 & 0 & 0 \end{pmatrix}$$

and its ideal of 7×7 minors is $\langle \omega_{11}^2, \omega_{11}\omega_{14}, \omega_{14}^2 \rangle$. As long as $\omega_{11}, \omega_{14} \neq 0$, then the fibers $\mathcal{F}(\Lambda, \Omega)$ are finite so ϕ_G is locally identifiable.

In fact, it is known that ϕ_G is identifiable when G is acyclic and has no bidirected edges. We end this background section with a statement of this useful theorem.

Theorem 2.23 (Theorem 7.2, [14]). If $G = (V, D, \emptyset)$ is an acyclic digraph, then ϕ_G is injective.

Chapter 3

Steady-state Degree of Chemical Reaction Networks

The work in this chapter is joint work with Dr. Jane Coons and Dr. Elizabeth Gross. The reader can find a preprint available on the arXiv [7].

3.1 Introduction

In this chapter, we use a different factorization of the mass-action system:

$$\frac{d\mathbf{x}}{dt} = Y A_{\kappa}^t \mathbf{x}^Y \quad (3.1)$$

where Y is a matrix whose columns are the complexes of the network and A_{κ} has off diagonal entries equal to k_{ij} and its row sums are zero. Define the *species-to-rate* matrix Σ to be the matrix product $Y A_{\kappa}^t$.

The interest is in chemical reaction networks where the steady-state ideal

is a binomial ideal. Occasionally the differential equations arising from mass-action kinetics on the network are themselves binomial, as is the case for the network in Figure 2.1. However it can also happen that these differential equations are not binomial, but ideal combinations of them are so that their steady-state ideal is generated by binomials. In this case, we say that the network has *binomial steady-states*. The following condition, introduced by Perez-Millan, Dickenstein, Shiu, and Conradi in [29], is a sufficient condition for the network to have binomial steady-states.

Condition 3.1. For a chemical reaction system given by a network G with m complexes and reaction rate constants κ_{ij} , let Σ denote its complex-to-species rate matrix, and set $d = \dim(\ker(\Sigma))$. We say that the chemical reaction system satisfies Condition 3.1, if there exists a partition I_1, \dots, I_d of $\{1, \dots, m\}$ and a basis $\mathbf{b}^1, \dots, \mathbf{b}^d$ of $\ker(\Sigma)$ with $\text{supp}(\mathbf{b}^i) = I_i$.

We will refer to networks as *PDSC networks* if they satisfy Condition 3.1, since PDSC are the initials of the authors of [29] where this condition was introduced. These authors prove the following result about PDSC networks.

Theorem 3.2 ([29], Theorem 3.3). Let G be a PDSC network as described in Condition 3.1. Then the steady-state ideal I_G is generated by the binomials of the form

$$b_{j_1}^j \mathbf{x}^{\mathbf{y}_{j_2}} - b_{j_2}^j \mathbf{x}^{\mathbf{y}_{j_1}}$$

for all $j_1, j_2 \in I_j$ and all $j \in [d]$.

Note that for a fixed $j \in [d]$, the binomials of the form $b_{j_1}^j \mathbf{x}^{\mathbf{y}_{j_2}} - b_{j_2}^j \mathbf{x}^{\mathbf{y}_{j_1}}$

for $j_1, j_2 \in I_j$ are generated by the $\#I_j - 1$ binomials

$$b_{j'}^j \mathbf{x}^{y_{j_2}} - b_{j_2}^j \mathbf{x}^{y_{j'}}$$

where j' is fixed and $j_2 \in I_j \setminus \{j'\}$. This observation yields the following corollary.

Corollary 3.3. Let G be a PDSC network with m complexes and with $\dim(\ker(\Sigma)) = d$. Then I_G has a generating set consisting of $m - d$ binomials.

3.2 Mixed Volumes of Partitionable Binomial Networks

Now we will focus on a specific class of binomial networks, particularly *partitionable networks*, and we show that, for these networks, computing the mixed volume reduces to computing the volume of a single mixed cell. We further show that one need not actually find such a mixed cell – in fact, in these cases, the mixed volume can be computed without computing a fine mixed subdivision. In order to define partitionable networks, we need the following algebraic notion of multihomogeneity.

Definition 3.4. Let I be an ideal in $\mathbb{K}[x_1, \dots, x_s]$. Let $\mathbf{w}_1, \dots, \mathbf{w}_k \in \mathbb{Z}^s$ be integer weight vectors. Then I is *multihomogeneous* with respect to the *multigrading* specified by $\mathbf{w}_1, \dots, \mathbf{w}_k$ if it has a generating set f_1, \dots, f_{s-k} such that for each $f_i = \sum_{\mathbf{a} \in \mathcal{A}_i} \beta_{\mathbf{a}} \mathbf{x}^{\mathbf{a}}$, we have $\mathbf{a} \cdot \mathbf{w}_j = \mathbf{b} \cdot \mathbf{w}_j$ for all $j \in [k]$ and $\mathbf{a}, \mathbf{b} \in \mathcal{A}_i$.

We note that multihomogeneity with respect to $\mathbf{w}_1, \dots, \mathbf{w}_k$ is a property of $\text{span}\{\mathbf{w}_1, \dots, \mathbf{w}_k\}$ and does not depend on the choice of spanning set of this vector space. Indeed, an ideal is multihomogenous with respect to $\mathbf{w}_1, \dots, \mathbf{w}_k$ if and only if it is homogeneous with respect to the weight order specified by any \mathbf{w} in their span.

We can now define a *partitionable network*, where the structure of the conservation law vectors leads to very nice geometry on the level of mixed volumes.

Definition 3.5. A network G is *partitionable* if

1. there are 0/1 vectors $\mathbf{w}_1, \dots, \mathbf{w}_k$ with disjoint support such that the linear space of all conservation laws of G is equal to $\text{span}\{\mathbf{w}_1, \dots, \mathbf{w}_k\}$ and
2. the steady-state ideal is multihomogeneous with respect to the multi-grading specified by the conservation law vectors.

Remark. The multihomogeneity condition for a network to be partitionable has a nice geometric interpretation. This condition is equivalent to the affine hull of the Newton polytope $\text{Newt}(f_i)$ being parallel to the stoichiometric subspace for each generator f_i of the steady-state ideal.

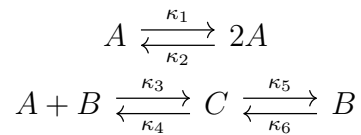
Observe that the first of the conditions in Definition 3.5 is the more restrictive one; in the proof of Theorem 3.8, it places significant restrictions on the form of the mixed cells that can appear in a fine mixed subdivision. The second condition is more mild. In particular, it is satisfied if the evaluations of a conservation law vector on each complex are equal. Notably, the undi-

rected graph underlying the network is connected; in this case, the network is referred to as *weakly connected*.

Proposition 3.6. If G is weakly connected, then its steady-state ideal I_G is multihomogeneous with respect to the multigrading specified by the conservation law vectors.

Proof. Let G be a weakly connected network with complexes $\mathbf{y}_1, \dots, \mathbf{y}_m$ and conservation law vectors $\mathbf{w}_1, \dots, \mathbf{w}_k$. Then by definition of a conservation law vector, for each reaction $\mathbf{y}_i \rightarrow \mathbf{y}_j$ and each conservation law vector \mathbf{w}_ℓ , we have $\mathbf{y}_i \cdot \mathbf{w}_\ell = \mathbf{y}_j \cdot \mathbf{w}_\ell$. Moreover, since G is weakly connected, there is an undirected path between each pair of complexes. Thus this equality holds for any pair of complexes \mathbf{y}_i and \mathbf{y}_j and any conservation law vector \mathbf{w}_ℓ . Every term of the steady-state equations $\frac{d\mathbf{x}}{dt} = 0$ that generate I_G is of the form $\mathbf{x}^{\mathbf{y}_i}$ for some complex \mathbf{y}_i . Thus the steady-state equations form a generating set of I_G that is multihomogeneous with respect to the multigrading specified by the conservation law vectors. \square

Example 3.7. As a non-example, the Edelstein network



is not partitionable. It has one conservation law vector $\mathbf{w} = (0, 1, 1)$ and if we consider the two exponent vectors $\mathbf{a} = (2, 0, 0)$ and $\mathbf{b} = (1, 1, 0)$ of the polynomial $f_A(\mathbf{x}) = \kappa_1 x_A - \kappa_2 x_A^2 - \kappa_3 x_A x_B + \kappa_4 x_C$, we compute $\mathbf{a} \cdot \mathbf{w} = 0$ while $\mathbf{b} \cdot \mathbf{w} = 1$.

The main result of this section is the following characterization of the mixed volume of a partitionable binomial reaction network. In particular, we find that any fine mixed subdivision of the Minkowski sum of the Newton polytopes of such a network has at most one cell of type $(1, \dots, 1)$. This allows us to easily compute the mixed volume of such a network, since if a type $(1, \dots, 1)$ cell exists, then the mixed volume is the volume of this single cell. If no such mixed cell exists, then the mixed volume is zero.

Theorem 3.8. Let G be a partitionable binomial network with s species and k conservation law vectors $\mathbf{w}_1, \dots, \mathbf{w}_k$ with disjoint support. Suppose that its steady-state ideal has a binomial generating set f_1, \dots, f_{s-k} with exactly $s - k$ elements. Then any fine mixed subdivision of $\sum_{i=1}^{s-k} \text{Newt}(f_i) + \sum_{j=1}^k \text{Newt}(\mathbf{w}_j \cdot \mathbf{x} - c_j)$ has at most one cell of type $(1, \dots, 1)$. This cell, if it exists, is a translate of some parallelotope of the form

$$\sum_{i=1}^{s-k} \text{Newt}(f_i) + \sum_{j=1}^k \text{conv}(\mathbf{0}, \mathbf{e}_{\alpha_j}),$$

where α_j is in the support of \mathbf{w}_j for all j .

Before we prove Theorem 3.8, we require the following well-known proposition regarding the Minkowski sums of a polytope with two different edges.

Proposition 3.9. Let P and Q be d -dimensional polytopes in \mathbb{R}^d that share a facet F . Suppose further that F is the face of both that maximizes the same linear functional \mathbf{a} . Then P and Q intersect on their interiors.

Proof. We have that $F = \{\mathbf{x} \in P \mid \mathbf{a} \cdot \mathbf{x} = b\} = \{\mathbf{x} \in Q \mid \mathbf{a} \cdot \mathbf{x} = b\}$ and that P and Q are contained in the closed halfspace $\{\mathbf{x} \mid \mathbf{a} \cdot \mathbf{x} \leq b\}$. Moreover, F

is a facet of both polytopes. So we may write minimal H-representations

$$P = \{\mathbf{x} \mid A\mathbf{x} \leq \mathbf{b}\} \quad \text{and} \quad Q = \{\mathbf{x} \mid C\mathbf{x} \leq \mathbf{d}\}$$

where the first rows of A and C , \mathbf{a}_1 and \mathbf{c}_1 respectively, are both equal to \mathbf{a} and the first entries of \mathbf{b} and \mathbf{d} are both b . Since F is a facet, we may further assume that for all $i > 1$ and all $\mathbf{x} \in F$, $\mathbf{a}_i \cdot \mathbf{x} < b_i$ and $\mathbf{c}_i \cdot \mathbf{x} < d_i$.

Let $\mathbf{z} \in \text{relint}(F)$. We construct an $\epsilon > 0$ such that $\mathbf{z} - \epsilon \mathbf{a}^t \in \text{int}(P) \cap \text{int}(Q)$. Consider the rows $\mathbf{a}_i, \mathbf{c}_j$ of A and C respectively for $i, j > 1$. Let $\epsilon > 0$ be such that $-\epsilon \mathbf{a}_i \cdot \mathbf{a}^t < b_i - \mathbf{a}_i \cdot \mathbf{z}$ and $-\epsilon \mathbf{c}_j \cdot \mathbf{a}^t < d_j - \mathbf{c}_j \cdot \mathbf{z}$ for all $i, j > 1$. Such an ϵ exists since $b_i - \mathbf{a}_i \cdot \mathbf{z}$ and $d_j - \mathbf{c}_j \cdot \mathbf{z}$ are strictly positive for all $i, j > 1$. Then

$$\mathbf{z} - \epsilon \mathbf{a}^t \in \{\mathbf{x} \mid A\mathbf{x} < \mathbf{b}\} \cap \{\mathbf{x} \mid C\mathbf{x} < \mathbf{d}\},$$

which is exactly the intersection of the interiors of P and Q , as needed. \square

Proof of Theorem 3.8. Since the mixed volume is translation invariant, we replace each $\text{Newt}(f_i)$ with its translation to the origin, $P_i := \text{conv}(\mathbf{0}, \mathbf{y}_1^{(i)} - \mathbf{y}_2^{(i)})$, where $f_i = \mathbf{x}^{\mathbf{y}_1^{(i)}} - \mathbf{x}^{\mathbf{y}_2^{(i)}}$. Let $P = \sum_{i=1}^{s-k} P_i + \sum_{j=1}^k \text{Newt}(\mathbf{w}_j \cdot \mathbf{x} - c_j)$. Each polytope P_i is a line segment since f_i is a binomial. Thus, for any fine mixed subdivision, a mixed cell of type $(1, \dots, 1)$ must have each P_i as a summand.

Further, note that there are two types of edges of each simplex $W_j := \text{Newt}(\mathbf{w}_j \cdot \mathbf{x} - c_j)$; they are of the form $\text{conv}(\mathbf{0}, \mathbf{e}_\alpha)$ or $\text{conv}(\mathbf{e}_\alpha, \mathbf{e}_\beta)$ where α and β are in the support of \mathbf{w}_j . For all $j \in [k]$, if α belongs to the support

of \mathbf{w}_j , then since G is partitionable, \mathbf{e}_α belongs to the linear space

$$\bigcap_{\substack{h=1 \\ h \neq j}}^k \{\mathbf{p} \mid \mathbf{w}_h \cdot \mathbf{p} = 0\}.$$

Moreover, since G is partitionable, the steady-state ideal I_G is multihomogeneous with respect to the multigrading specified by the conservation law vectors. Since I_G contains no monomials, this implies that each f_i is multihomogeneous with respect to this multigrading as well. Thus $\mathbf{w}_h \cdot (\mathbf{y}_1^{(i)} - \mathbf{y}_2^{(i)}) = 0$ for all $h \in [k]$ and $i \in [s - k]$.

Let Q be a type $(1, \dots, 1)$ mixed cell of a fine mixed subdivision of P . Then $Q = \sum_{i=1}^{s-k} P_i + \sum_{j=1}^k E_j$ where each E_j is an edge of W_j . For the sake of contradiction, suppose that $E_j = \text{conv}(\mathbf{e}_\alpha, \mathbf{e}_\beta)$ for some j . Then $\sum_{i=1}^{s-k} P_i + E_j$ lies in the codimension k affine linear space

$$\{\mathbf{p} \mid \mathbf{w}_j \cdot \mathbf{p} = 1\} \cap \bigcap_{\substack{h=1 \\ h \neq j}}^k \{\mathbf{p} \mid \mathbf{w}_h \cdot \mathbf{p} = 0\}.$$

So it has dimension less than or equal to $s - k$. Thus Q has dimension less than or equal to $s - 1$, which contradicts that it is a maximal cell of a fine mixed subdivision.

Thus all mixed cells of type $(1, \dots, 1)$ are of the form $\sum_{i=1}^{s-k} P_i + \sum_{j=1}^k \text{conv}(\mathbf{0}, \mathbf{e}_{\alpha_j})$ where α_j belongs to the support of \mathbf{w}_j . Let E_{α_j} denote $\text{conv}(\mathbf{0}, \mathbf{e}_{\alpha_j})$.

Now suppose that Q_1 and Q_2 are distinct mixed cells of this form. They must differ by at least one summand corresponding to edges of some W_j . Without loss of generality, suppose that this is \mathbf{w}_1 and that the summand

associated to \mathbf{w}_1 in Q_1 is E_1 and the summand associated to \mathbf{w}_1 in Q_2 is E_2 . Consider the face of P that minimizes the linear functionals $\mathbf{w}_j \cdot \mathbf{p}$ for all $j = 2, \dots, k$. This face is $F = \sum_{i=1}^{s-k} P_i + W_1$. The fine mixed subdivision \mathcal{S} of P restricts to a subdivision \mathcal{S}' of this face via intersection. Moreover, we have $Q_1 \cap F = \sum_{i=1}^{s-k} P_i + E_1$ and $Q_2 \cap F = \sum_{i=1}^{s-k} P_i + E_2$.

Now consider these polytopes in the ambient linear space, $\{\mathbf{p} \mid \mathbf{w}_j \cdot \mathbf{p} = 0, j = 2, \dots, k\}$. The face F is contained in the hyperplane $\{\mathbf{w}_1 \cdot \mathbf{p} = 0\}$ and E_1 and E_2 both lie in the positive halfspace defined by $\mathbf{w}_1 \cdot \mathbf{p} \geq 0$. So by Proposition 3.9, we have that $\text{relint}(\sum_{i=1}^k P_i + E_1) \cap \text{relint}(\sum_{i=1}^k P_i + E_2)$ is nonempty. Moreover, these two polytopes are not equal. So they cannot belong to the same subdivision of F . Hence, Q_1 and Q_2 cannot belong to the same subdivision of P . Thus a fine mixed subdivision of P has at most one mixed cell of type $(1, \dots, 1)$ and it has the desired form if it exists. \square

Consider a partitionable binomial reaction network as in the statement of Theorem 3.8. We have shown that any fine mixed subdivision of the Minkowski sum of its Newton polytopes has at most one mixed cell of type $(1, \dots, 1)$ and described the form of this cell if it exists. Let Π denote this parallelotope. If one knows the edges of each Newton polytope that are its Minkowski summands, then its volume can be computed as the determinant of a matrix.

Lemma 3.10. Let G be as in the statement of Theorem 3.8 and suppose that

$$\Pi = \sum_{i=1}^{s-k} \text{Newt}(f_i) + \sum_{j=1}^k \text{conv}(\mathbf{0}, \mathbf{e}_{\alpha_j})$$

be the unique type $(1, \dots, 1)$ cell of a fine mixed subdivision of the Newton

polytopes where each $f_i = \mathbf{x}^{\mathbf{y}_1^{(i)}} - \mathbf{x}^{\mathbf{y}_2^{(i)}}$ and where α_j is in the support of \mathbf{w}_j . Then the mixed volume of the steady-state system f_1, \dots, f_{s-k} augmented by the partitionable conservation laws the absolute value of the determinant of the $s \times s$ matrix with columns \mathbf{e}_{α_j} for $j \in [k]$ and $\mathbf{y}_1^{(i)} - \mathbf{y}_2^{(i)}$ for $i \in [s-k]$

Proof. Suppose that this mixed volume is non-zero. The volume of a polytope is invariant under translation. To compute the volume of the parallelotope Π , we translate it to the origin by replacing the edge $\text{Newt}(f_i) = \text{conv}(\mathbf{y}_1^{(i)}, \mathbf{y}_2^{(i)})$ with $\text{conv}(\mathbf{0}, \mathbf{y}_1^{(i)} - \mathbf{y}_2^{(i)})$. Then this determinant is the standard formula for the normalized volume of such a parallelotope. By Theorem 3.8, Π is the only mixed cell of type $(1, \dots, 1)$ in a fine mixed subdivision of P . Thus by Theorem 1.22, the mixed volume of G is the volume of Π . \square

We conclude this discussion by noting that this determinant does not depend on the choice of the coordinates α_j in the support of \mathbf{w}_j . So in fact, one can compute the mixed volume of a partitionable binomial reaction network via a simple determinant calculation without computing a fine mixed subdivision. In order to prove this, we state the following lemma.

Lemma 3.11. Let $\mathbf{r}_1, \dots, \mathbf{r}_{k+1}$ be s -dimensional row vectors that sum to the zero vector. Let $\mathbf{q}_1, \dots, \mathbf{q}_{s-k}$ be arbitrary s -dimensional row vectors. Let R_i denote the $s \times s$ matrix with rows $\mathbf{r}_1, \dots, \mathbf{r}_{k+1}, \mathbf{q}_1, \dots, \mathbf{q}_{s-k}$ with \mathbf{r}_i excluded. Then $\det(R_i) = (-1)^{i-j} \det(R_j)$ for any $i, j \in [k+1]$.

Proof. For any i, j , we have

$$\mathbf{r}_i = - \sum_{\substack{\ell=1 \\ \ell \neq i}}^{k+1} \mathbf{r}_\ell.$$

Replacing \mathbf{r}_i with this expression in R_j and expanding using multilinearity and the alternating property of the determinant yields that $\det(R_j) = -\det(R_j^{(i)})$, where $R_j^{(i)}$ is obtained from R_j by replacing \mathbf{r}_j with \mathbf{r}_i . Then using $i - j - 1$ adjacent row swaps to put \mathbf{r}_i in the i th position yields R_i . So $\det(R_j) = (-1)^{i-j} \det(R_i)$, as needed. \square

Theorem 3.12. Let G be a partitionable binomial reaction network with partitionable conservation law vectors $\mathbf{w}_1, \dots, \mathbf{w}_k$ and exactly $s - k$ defining binomials f_i supported on exponent vectors $\mathbf{y}_1^{(i)}$ and $\mathbf{y}_2^{(i)}$. Then the mixed volume of the steady-state system f_1, \dots, f_{s-k} augmented by the partitionable conservation laws is either 0 or the absolute value of the determinant of *any* matrix with columns $\mathbf{y}_1^{(i)} - \mathbf{y}_2^{(i)}$ for all $i \in [s - k]$ and \mathbf{e}_{α_j} for $\alpha_j \in \text{supp}(\mathbf{w}_j)$ for each $j \in [k]$.

Proof. Suppose that the system $f_i(\mathbf{x}) = 0$ for $i \in [s - k]$ and $\mathbf{w}_j \cdot \mathbf{x} = c_j$ for $j \in [k]$ has nonzero mixed volume. Then any fine mixed subdivision of p has a type $(1, \dots, 1)$ cell, and by Theorem 3.8, this cell is unique and of the form

$$\Pi = \sum_{i=1}^{s-k} \text{Newt}(f_i) + \sum_{j=1}^k \text{conv}(\mathbf{0}, \mathbf{e}_{\alpha_j}).$$

Let M_α denote the matrix with columns $\mathbf{y}_1^{(i)} - \mathbf{y}_2^{(i)}$ for all $i \in [s - k]$ and \mathbf{e}_{α_j} for $j \in [k]$. Then by Lemma 3.10, the mixed volume of G is equal to $\pm \det(M_\alpha)$.

It remains to show that if we pick $\beta_j \in \text{supp}(\mathbf{w}_j)$ for each j , the corresponding matrix has the same determinant up to absolute value; that is, that $\det M_\alpha = \pm \det M_\beta$. Consider the $s \times (s - k)$ matrix M with columns

$\mathbf{y}_1^{(i)} - \mathbf{y}_2^{(i)}$. Let $\mathbf{r}_1, \dots, \mathbf{r}_s$ be its rows. Note that for each $j \in [k]$, we have

$$\sum_{\ell \in \text{supp}(\mathbf{w}_j)} \mathbf{r}_\ell = 0.$$

Let M'_α denote the matrix obtained by deleting rows $\mathbf{r}_{\alpha_1}, \dots, \mathbf{r}_{\alpha_s}$ from M , and similarly for M'_β . Then by repeatedly applying Laplace expansion along the columns of the form \mathbf{e}_{α_j} , we see that $\det M_\alpha = \pm \det M'_\alpha$, and similarly, that $\det M_\beta = \pm \det M'_\beta$. Moreover, by applying Lemma 3.11 s times to the block of rows $\{\mathbf{r}_\ell \mid \ell \in \text{supp}(\mathbf{w}_j)\}$ at the j th step of the Laplace expansion, we see that

$$\det(M'_\alpha) = \pm \det(M'_\beta),$$

as needed. □

3.3 Cycles with Binomial Steady-States

In this section, we investigate the directed cycles, or *cycle networks*, that satisfy the PDSC Condition. We give a characterization of these cycles in terms of edge colorings of the cycle. Then we apply the results of Section 3 to some examples of cycles with binomial steady-states and compute their mixed volumes.

Let G be a cycle network with m complexes, that is, defined by the reactions $\mathbf{y}_i \xrightarrow{\kappa_i} \mathbf{y}_{i+1}$ where the indices are taken modulo the set $[m] = \{1, 2, \dots, m\}$. Let $d = \dim \ker \Sigma$ where $\Sigma = Y^t A_\kappa^t$. Since we are fixing the

structure of the reaction graph G , the Laplacian matrix has the form

$$A_{\kappa}^t = \begin{pmatrix} -\kappa_1 & & & & & & & \kappa_m \\ \kappa_1 & -\kappa_2 & & & & & & \\ & \kappa_2 & -\kappa_3 & & & & & \\ & & & \ddots & & & & \\ & & & & & & -\kappa_{m-1} & \\ & & & & & & \kappa_{m-1} & -\kappa_m \end{pmatrix}$$

which has nontrivial kernel; indeed, it contains the non-zero vector $\mathbf{x}_{\kappa} = (\kappa_1^{-1}, \dots, \kappa_m^{-1})^t$. Thus, for cycle networks, the dimension d of the kernel of $\Sigma = Y^t A_{\kappa}^t$ is always at least 1.

Given a coloring of the edges of G , $\lambda : E(G) \rightarrow C$, and a “color” $\ell \in C$, the subgraph of G induced by all edges of color ℓ , denoted $G[\ell]$ is a disjoint union of directed paths if $|C| > 1$ and G if $|C| = 1$. Let $H(\ell)$ denote the set of all source vertices of $G[\ell]$ and let $T(\ell)$ denote the set of all sink vertices of $G[\ell]$. Note that in the case $|C| = 1$, the sets $H(\ell)$ and $T(\ell)$ are both empty. Given a subset S of the complexes of G , we shall write $\mathbb{1}_S$ to denote the m -dimensional indicator vector for S .

Theorem 3.13. Let G be a directed cycle. Then G is a PDSC network if and only if there exists a surjective coloring $\lambda : E(G) \rightarrow [d]$ such that for all $\ell \in [d]$,

$$\sum_{\mathbf{y} \in H(\ell)} \mathbf{y} = \sum_{\mathbf{y} \in T(\ell)} \mathbf{y}.$$

Proof. Let $\lambda : E(G) \rightarrow [d]$ be a surjective coloring of the edges of G such that for all $\ell \in [d]$, $\sum_{\mathbf{y} \in H(\ell)} \mathbf{y} = \sum_{\mathbf{y} \in T(\ell)} \mathbf{y}$. Then the difference of indicator

vectors $\mathbb{1}_{H(\ell)} - \mathbb{1}_{T(\ell)}$ belongs to $\ker Y^t$ for all $\ell \in [d]$. This is equal to the image of the vector \mathbf{b}^ℓ under A_κ^t where \mathbf{b}^ℓ is defined by

$$b_i^\ell = \begin{cases} \kappa_i^{-1} & \text{if } \lambda(\mathbf{y}_i \rightarrow \mathbf{y}_{i+1}) = \ell \\ 0 & \text{otherwise.} \end{cases}$$

Indeed, if \mathbf{y}_i is the source of a path in $G[\ell]$, then $b_i^\ell = \kappa_i^{-1}$ and $b_{i-1}^\ell = 0$. So the i th entry of $A_\kappa^t \mathbf{b}^\ell$ is -1 . Similarly, if \mathbf{y}_i is the sink of a path in $G[\ell]$, then $b_i^\ell = 0$ and $b_{i-1}^\ell = \kappa_{i-1}^{-1}$. So the i th entry of $A_\kappa^t \mathbf{b}^\ell$ is 1 . If \mathbf{y}_i is an interior node on a path in $G[\ell]$, then $b_i^\ell = \kappa_i^{-1}$ and $b_{i-1}^\ell = \kappa_{i-1}^{-1}$, so that the i th entry of $A_\kappa^t \mathbf{b}^\ell$ is 0 . Finally if \mathbf{y}_i does not belong to $G[\ell]$, then \mathbf{y}_{i-1} either is also not in $G[\ell]$ or is a sink of a path in $G[\ell]$. Hence we have $b_i^\ell = b_{i-1}^\ell = 0$, and the i th entry of $A_\kappa^t \mathbf{b}^\ell$ is 0 .

The vectors $\mathbf{b}^1, \dots, \mathbf{b}^d$ have disjoint support since each complex has exactly one outgoing end. Thus they are linearly independent. Moreover, they form a basis for $\ker \Sigma$ as they comprise d distinct vectors. Thus G satisfies Condition 3.1.

Now suppose that G satisfies Condition 3.1 and let $\mathbf{b}^1, \dots, \mathbf{b}^d$ be a basis for $\ker \Sigma$ with disjoint support. In particular, we know that $\mathbf{x}_\kappa = (\kappa_1^{-1}, \dots, \kappa_m^{-1})^t$ is in $\ker \Sigma$ as it belongs to $\ker A_\kappa^t$. So it is in the span of $\mathbf{b}^1, \dots, \mathbf{b}^d$. Thus, after rescaling each \mathbf{b}^ℓ , we have that if $j \in \text{supp}(\mathbf{b}^\ell)$, then $b_j^\ell = \kappa_j^{-1}$.

Color the edges of G by letting the edge $\mathbf{y}_i \rightarrow \mathbf{y}_{i+1}$ have color ℓ if and only if $i \in \text{supp}(\mathbf{b}^\ell)$. Then $A_\kappa^t \mathbf{b}^\ell = \mathbb{1}_{H(\ell)} - \mathbb{1}_{T(\ell)}$. Since $\mathbf{b}^\ell \in \ker \Sigma$, we must have that $\mathbb{1}_{H(\ell)} - \mathbb{1}_{T(\ell)} \in \ker Y^t$. Hence we have $\sum_{\mathbf{y} \in H(\ell)} \mathbf{y} = \sum_{\mathbf{y} \in T(\ell)} \mathbf{y}$, as needed. \square

The above proof uncovers another key fact about PDSC cycle networks. In particular, when the reaction rate constants κ_i are positive, these networks trivially satisfy another condition from [29], which we restate below.

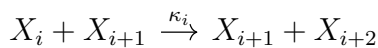
Condition 3.14 ([29], Condition 3.4). Consider a chemical reaction system given by the PDSC network G with m complexes and reaction rate constants κ_{ij} . There is a partition I_1, \dots, I_d of $[m]$ and a basis $\mathbf{b}^1, \dots, \mathbf{b}^d$ of $\ker \Sigma$ with $\text{supp} \mathbf{b}^i = I_i$. We say that the chemical reaction system additionally satisfies Condition 3.14 if for all $j \in [d]$, the nonzero entries of \mathbf{b}^j have the same sign, that is, if

$$\text{sign}(b_{j_1}^j) = \text{sign}(b_{j_2}^j) \quad \text{for all } j_1, j_2 \in I_j, \text{ for all } 1 \leq j \leq d.$$

Theorem 3.8 of [29] shows that this condition is necessary for a PDSC network to have a positive steady-state. The basis vectors $\mathbf{b}^1, \dots, \mathbf{b}^d$ from the proof of Theorem 3.13 are of a special form. In particular, when the reaction rate constants κ_i are positive, their nonzero entries are all positive. This shows that PDSC cycle networks automatically satisfy Condition 3.14.

Corollary 3.15. Let G be a directed cycle. If G is a PDSC network, then the chemical reaction system given by G satisfies Condition 3.14.

Example 3.16 (Species-overlapping cycles). An instance of PDSC cycle networks are what we call *species-overlapping cycles*, denoted SOC_m where $m \geq 3$. This one-parameter family of cycle networks are defined by reactions of the form



for $i = 1, \dots, m$ where the indices are taken modulo the set $[m] = \{1, \dots, m\}$.

For example, when $m = 4$ we get the network seen in Figure 3.1.

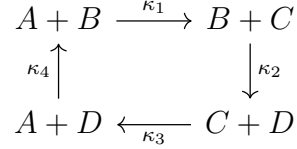


Figure 3.1: A four-cycle with positive binomial steady-states.

Note that the system of ordinary differential equations arising from these cycles is binomial. Our claim is that for $m \geq 3$ these networks are also indeed PDSC networks. When m is odd, the matrix

$$Y^t = \begin{pmatrix} 1 & & & & 1 \\ 1 & 1 & & & \\ & 1 & 1 & & \\ & & & \ddots & \\ & & & & 1 \end{pmatrix} = \left(\mathbf{e}_1 + \mathbf{e}_2 \quad \mathbf{e}_2 + \mathbf{e}_3 \quad \cdots \quad \mathbf{e}_{m-1} + \mathbf{e}_m \quad \mathbf{e}_1 + \mathbf{e}_m \right)$$

has full rank and hence $x_{\kappa} = (\kappa_1^{-1}, \kappa_2^{-1}, \dots, \kappa_m^{-1})^t$ generates the kernel of Σ . Thus, $d = 1$ and by Theorem 3.13, SOC_m for odd m is a PDSC network since $H(\ell) = T(\ell) = \emptyset$. Else if m is even, then $d = 2$ and a surjective coloring of the edges of the network is given as follows:

$$\lambda(\mathbf{y}_i \rightarrow \mathbf{y}_{i+1}) = \begin{cases} 1, & \text{if } i \text{ is odd} \\ 2, & \text{if } i \text{ is even.} \end{cases}$$

With this coloring, we have $H(1) = T(2)$, $T(1) = H(2)$, and satisfy the

following condition:

$$\begin{aligned}
\sum_{\mathbf{y} \in H(1)} \mathbf{y} &= \mathbf{y}_2 + \mathbf{y}_4 + \cdots + \mathbf{y}_m \\
&= (\mathbf{e}_2 + \mathbf{e}_3) + (\mathbf{e}_4 + \mathbf{e}_5) + \cdots + (\mathbf{e}_m + \mathbf{e}_1) \\
&= (\mathbf{e}_1 + \mathbf{e}_2) + (\mathbf{e}_3 + \mathbf{e}_4) + \cdots + (\mathbf{e}_{m-1} + \mathbf{e}_m) \\
&= \mathbf{y}_1 + \mathbf{y}_3 + \cdots + \mathbf{y}_{m-1} \\
&= \sum_{\mathbf{y} \in T(1)} \mathbf{y}.
\end{aligned}$$

Thus, by Theorem 3.13 SOC_m satisfies Condition 3.1 for even m .

These networks are also partitionable and we compute the mixed volume of their natural system of equations as in Theorem 3.12.

Theorem 3.17. Let $m \geq 3$. The cycle networks SOC_m are partitionable. The mixed volumes of the associated systems

$$\begin{cases} f_i &= \kappa_{i-2}x_{i-2}x_{i-1} - \kappa_i x_i x_{i+1} \quad , \text{ for } i = 1, \dots, m-1 \\ 0 &= x_1 + x_2 + \cdots x_m + c \end{cases}$$

for odd m and

$$\begin{cases} f_i &= \kappa_{i-2}x_{i-2}x_{i-1} - \kappa_i x_i x_{i+1} \quad , \text{ for } i = 1, \dots, m-2 \\ 0 &= x_1 + x_3 + \cdots x_{m-1} + c_1 \\ 0 &= x_2 + x_4 + \cdots x_m + c_2 \end{cases}$$

for even m are 1 and $\frac{m}{2}$, respectively.

Proof. For the cycle network SOC_m , the polynomials of the mass-action system (2.1) are $f_i = \kappa_{i-2}x_{i-2}x_{i-1} - \kappa_i x_i x_{i+1}$ so $\text{Newt}(f_i) = \text{conv}\mathcal{A}_i$ where $\mathcal{A}_i = \{\mathbf{e}_{i-2} + \mathbf{e}_{i-1}, \mathbf{e}_i + \mathbf{e}_{i+1}\}$. We organize the proof based on the parity of m .

First suppose m is odd. Then the network SOC_m has one conservation law given by the conservation law vector $\mathbf{w} = \mathbb{1}$. Since each f_i is homogenous then $I = \langle f_1, \dots, f_{m-1} \rangle$ is multihomogenous with respect to the multigrading given by \mathbf{w} , hence SOC_m is partitionable. By Theorem 3.12 the mixed volume of SOC_m is the absolute value of the determinant of the matrix with columns \mathbf{e}_1 and $\mathbf{e}_{i-2} + \mathbf{e}_{i-1} - \mathbf{e}_i - \mathbf{e}_{i+1}$ for $i = 1, \dots, m-1$. Since one of the columns of this matrix is \mathbf{e}_1 , we focus on the determinant of the submatrix after removing this column and the first row. For $m = 3$, the submatrix is $\begin{pmatrix} 0 & -1 \\ 1 & 0 \end{pmatrix}$ which has determinant 1, as desired. For $m \geq 5$, the submatrix has an LU-factorization with

$$L = \left(\begin{array}{cccc|cc} & & & & & & & \mathbf{0} \\ & & & & & & & \\ \hline & & & & & & & \\ -1 & \cdots & (-1)^j \lceil j/2 \rceil & \cdots & \lceil (m-3)/2 \rceil & & 1 & 0 \\ -1 & \cdots & -(j \bmod 2) & \cdots & 0 & & 1/\lceil (m-3)/2 \rceil & 1 \end{array} \right)$$

and

$$U = \left(\begin{array}{c|cc} U_1 & & U_2 \\ \hline & \lceil (m-3)/2 \rceil & -1 \\ \mathbf{0} & 0 & 1/\lceil (m-3)/2 \rceil \end{array} \right)$$

where $I_{(m-3)\times(m-3)}$ is the $(m-3)\times(m-3)$ identity matrix and the i th row of $\begin{pmatrix} U_1 & U_2 \end{pmatrix}$ is $\mathbf{e}_{i+2} + \mathbf{e}_{i+3} - \mathbf{e}_i - \mathbf{e}_{i+1}$ except the last row is $\mathbf{e}_{m-1} - \mathbf{e}_{m-3} - \mathbf{e}_{m-2}$. Therefore, the mixed volume is $\det(L)\det(U) = (-1)^{m-3} = 1$.

Now suppose m is even. The network SOC_m has two conservation laws given by the vectors $\mathbf{w}_1 = \mathbf{e}_1 + \mathbf{e}_3 + \cdots + \mathbf{e}_{m-1}$ and $\mathbf{w}_2 = \mathbf{e}_2 + \mathbf{e}_4 + \cdots + \mathbf{e}_m$. Then for any i, j and $\mathbf{a}, \mathbf{b} \in \mathcal{A}_i$, $\mathbf{a} \cdot \mathbf{w}_j = \mathbf{b} \cdot \mathbf{w}_j = 1$ so $I = \langle f_1, \dots, f_{m-2} \rangle$ is multihomogeneous with respect to the conservation law vectors $\mathbf{w}_1, \mathbf{w}_2$ and hence SOC_m is partitionable. By Theorem 3.12 the mixed volume of SOC_m is the absolute value of the determinant of the matrix with columns $\mathbf{e}_1, \mathbf{e}_2$, and $\mathbf{e}_{i-2} + \mathbf{e}_{i-1} - \mathbf{e}_i - \mathbf{e}_{i+1}$ for $i = 1, \dots, m-2$. Since the first two columns are $\mathbf{e}_1, \mathbf{e}_2$, we focus on the determinant of the submatrix after removing the first two rows and columns. For $m = 4$, the submatrix is $\begin{pmatrix} 1 & -1 \\ 1 & 1 \end{pmatrix}$ which has determinant $\frac{m}{2} = 2$, as desired. For $m \geq 6$, up to a permutation matrix, we have the following LU-factorization with

$$L = \left(\begin{array}{c|cccc|c} 1 & & & & & 0 \\ \hline \mathbf{0} & & & & & \mathbf{0} \\ \hline 1 & -1 & \cdots & (-1)^j \lceil j/2 \rceil & \cdots & \lceil (m-4)/2 \rceil \\ \hline & & & & & 1 \end{array} \right)$$

and

$$U = \begin{pmatrix} 1 & \mathbf{0} & 1 \\ \mathbf{0} & U_1 & U_2 \\ 0 & \mathbf{0} & m/2 \end{pmatrix}$$

where the i th row of $\begin{pmatrix} U_1 & U_2 \end{pmatrix}$ is $\mathbf{e}_{i+2} + \mathbf{e}_{i+3} - \mathbf{e}_i - \mathbf{e}_{i+1}$ except the last two rows are $\mathbf{e}_{m-2} - \mathbf{e}_{m-4} - \mathbf{e}_{m-3}$ and $-\mathbf{e}_{m-3} - \mathbf{e}_{m-2}$. Thus, the mixed volume

of SOC_m for m even is $(-1)^{\frac{m-4}{2}} \frac{m}{2} = \frac{m}{2}$. □

Chapter 4

Weighted Tropical Fermat-Weber Points

This chapter is joint work with Shelby Cox and a preprint can be found on the Arxiv [9].

4.1 Introduction

In this section we set up the framework of the Fermat-Weber problem and introduce the algebraic and geometric tools that we use to study it.

4.1.1 Tropical polynomials and regular subdivisions

Tropical Arithmetic

In the tropical max-plus semi-ring $(\mathbb{R} \cup \{-\infty\}, \oplus, \odot)$, tropical addition \oplus and tropical multiplication \odot are defined by

$$a \oplus b = \max\{a, b\}, \quad a \odot b = a + b \quad \text{where } a, b \in \mathbb{R}.$$

The multiplicative identity is 0, and the additive identity is $-\infty$. These operations can be extended component-wise $\mathbb{R}^n/\mathbb{R}\mathbb{1}$. For vectors $\mathbf{v}, \mathbf{u} \in \mathbb{R}^n/\mathbb{R}\mathbb{1}$, the notation $\mathbf{v} \oplus \mathbf{u}$ and $\mathbf{v} \odot \mathbf{u}$ denotes component-wise max and addition, respectively. Tropical scalar multiplication of a vector amounts to adding a (classical) multiple of the all ones vector $\mathbb{1}_n$, namely $\lambda \odot \mathbf{v} = \lambda \mathbb{1} + \mathbf{v} = (\lambda + v_1, \dots, \lambda + v_n)$ for any $\lambda \in \mathbb{R}$.

Example 4.1. If $\mathbf{v}_1 = (1, 2, -3)$ and $\mathbf{v}_2 = (-5, 3, 2)$ are points in $\mathbb{R}^3/\mathbb{R}\mathbb{1}$,

then

$$\begin{aligned}\mathbf{v}_1 \oplus \mathbf{v}_2 &= (\max\{1, -5\}, \max\{2, 3\}, \max\{-3, 2\}) \\ &= (1, 3, 2) = (-1, 1, 0)\end{aligned}$$

$$\begin{aligned}\mathbf{v}_1 \odot \mathbf{v}_2 &= (1 - 5, 2 + 3, -3 + 2) \\ &= (-4, 5, -1)\end{aligned}$$

$$\begin{aligned}3 \odot v_2 &= (3 - 5, 3 + 3, 3 + 2) \\ &= (-2, 6, 5)\end{aligned}$$

Later it will be convenient to fix a specific representative of $v \in \mathbb{R}^n/\mathbb{R}\mathbf{1}$, namely the one where the sum of the coordinates is zero. We denote by H_0 the hyperplane where these points are located:

$$H_0 := \left\{ \mathbf{z} \in \mathbb{R}^n \mid \mathbf{z} \cdot \mathbf{1} = \sum_i z_i = 0 \right\} \subset \mathbb{R}^n.$$

Each point in $\mathbb{R}^n/\mathbb{R}\mathbf{1}$ has a unique representative in H_0 .

When we draw pictures in $\mathbb{R}^n/\mathbb{R}\mathbf{1}$, we will tropically scale points to have last coordinate zero, then project away the last coordinate and draw the point in \mathbb{R}^{n-1} . For example, $(3, 1, 2) \equiv (1, -1, 0)$ will be drawn in the plane at the location $(1, -1)$.

Tropical Polynomials

Let $\mathbf{x}, \mathbf{a} \in \mathbb{R}^n$, and define the tropical monomial: $\mathbf{x}^{\mathbf{a}} := \sum_{i=1}^n a_i x_i$. Note that when the entries of \mathbf{a} are non-negative integers:

$$x_1^{a_1} \odot \cdots \odot x_n^{a_n} = \underbrace{x_1 \odot \cdots \odot x_1}_{a_1 \text{ times}} \odot \cdots \odot \underbrace{x_n \odot \cdots \odot x_n}_{a_n \text{ times}},$$

which explains the notation. Note that for $\mathbf{a} \in \mathbb{R}^n$, $\mathbf{x}^{\mathbf{a}}$ is still a well-defined tropical function, but not a tropical polynomial.

Definition 4.2. Let $\mathbf{x} \in \mathbb{R}^n/\mathbb{R}1$. A *tropical signomial in \mathbf{x}* is a finite linear combination of tropical monomials, i.e.

$$f(\mathbf{x}) = \bigoplus_{\mathbf{a} \in A} \lambda_{\mathbf{a}} \odot \mathbf{x}^{\mathbf{a}}$$

where $A \subset \mathbb{R}_{\geq 0}^n$ is finite and $\lambda_{\mathbf{a}} \in \mathbb{R}$ for all $\mathbf{a} \in A$. If $A \subset \mathbb{Z}_{\geq 0}^n$, then $f(\mathbf{x})$ is a *tropical polynomial*.

Example 4.3. Let $f(x) = 1 \oplus 3 \odot x \oplus -1 \odot x^{\sqrt{2}}$. In terms of classical arithmetic operations:

$$f(x) = \max\{1, 3 + x, -1 + \sqrt{2}x\}.$$

The graph of $f(x)$ is depicted in 4.1; it has three linear pieces:

$$f(x) = \begin{cases} 1 & \text{if } x \leq -2 \\ 3 + x & \text{if } -2 \leq x \leq \frac{4}{\sqrt{2}-1} \\ -1 + \sqrt{2}x & \text{if } \frac{4}{\sqrt{2}-1} \leq x. \end{cases}$$

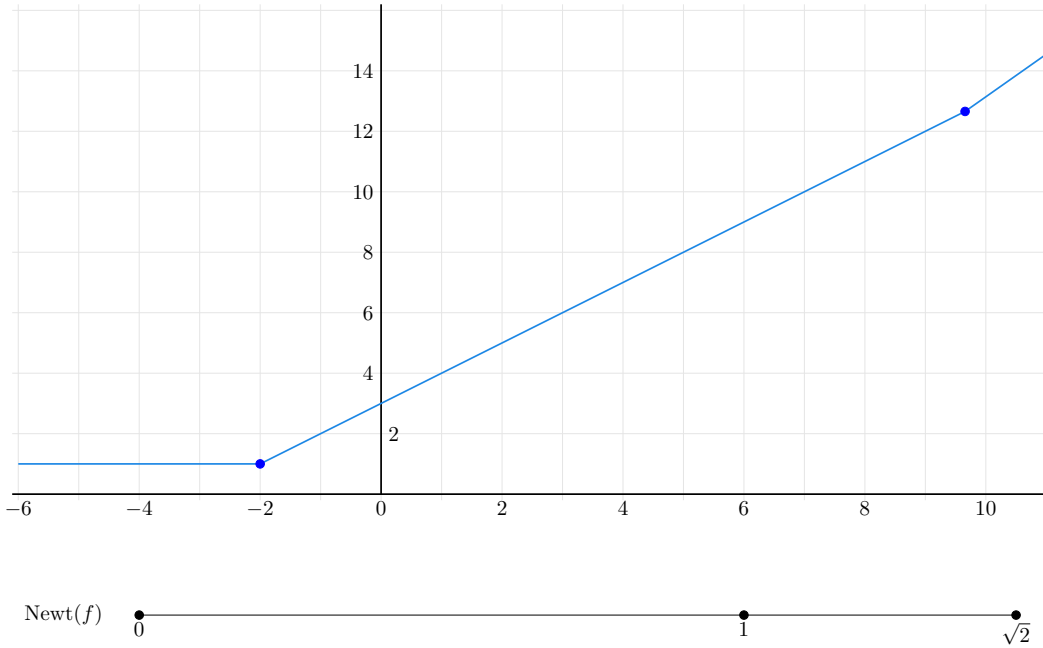


Figure 4.1: The graph of $f(x) = 1 \oplus 3 \odot x \oplus -1 \odot x^{\sqrt{2}}$. The connection to the Newton polytope of f is explained in 4.1.1.

Optimization

A tropical max-plus signomial is a piecewise linear, continuous, convex function on \mathbb{R}^n . For a convex function, any local minimum is a global minimum. This minimum can be identified by locating the tangent plane with zero slope, which we formalize using subgradients.

Definition 4.4 ([26, §3.1.5]). Given a convex function $f : \mathbb{R}^n \rightarrow \mathbb{R}$, the *subdifferential* of f at x is:

$$\partial_f(x) := \{u \in \mathbb{R}^n \mid \forall z \in \text{dom}(f), f(z) \geq f(x) + u^\top \cdot (z - x)\}. \quad (4.1)$$

A *subgradient* of f at x is any element of $\partial_f(x)$.

The subdifferential of any function is a closed convex set. If f is convex and differentiable at x , then the subdifferential of f at x is a singleton. In particular, if f is linear then the subdifferential contains only the slope of f . And if f is piecewise linear, then $\partial_f(x)$ is constant on the linear pieces of f .

Lemma 4.5 ([26, Theorem 3.1.15]). For any function f , the subdifferential at x contains $\bar{\mathbf{0}}$ if and only if x is a global minimizer for f .

Proof. By definition, $\bar{\mathbf{0}} \in \partial_f(x)$ if and only if

$$\forall z \in \text{dom}(f), f(z) \geq f(x) + \bar{\mathbf{0}}^\top \cdot (z - x) \iff \forall z \in \text{dom}(f), f(z) \geq f(x),$$

which is if and only if x is a global minimizer for f . □

Example 4.6. Let $f(x) = 1 \oplus 3 \odot x \oplus -1 \odot x^{\sqrt{2}}$. The subdifferential of $f(x)$ on each linear piece is the slope of that piece. The subdifferential at $x = -2$ is $\partial_f(-2) = [0, 1]$, and the subdifferential at $x = 4(1 + \sqrt{2})$ is $[1, \sqrt{2}]$. Note that 0 is in the subdifferential of the constant (left-most) linear piece, and this is where the global minimum of $f(x)$ is achieved. See 4.1.

Tropical Hypersurfaces

The results we stated for subgradients hold for any convex function. In this section we recall further results for tropical signomials. For a tropical polynomial $f : \mathbb{R}^n \rightarrow \mathbb{R}$, subdifferentials of linear pieces of f are encoded by a subdivision of $\text{Newt}(f)$. It is this connection that will allow us to convert the problem of optimizing f into a polyhedral geometry problem.

Definition 4.7. The *tropical vanishing set* or *tropical hypersurface* of a tropical signomial $f = \bigoplus_i c_i \odot x^{\alpha_i}$, denoted $\text{tropV}(f)$, is the set of $x \in \mathbb{R}^n$ for which the max in $f(x)$ is achieved at least twice.

$$\text{tropV}(f) = \{x \in \mathbb{R}^n \mid \max \text{ in } f(x) \text{ is achieved at least twice}\}. \quad (4.2)$$

Lemma 4.8. The tropical vanishing set of a product of real positive powers of polynomials, $f_i^{w_i}$, is (as a set) the union of tropical vanishing sets of the f_i . That is,

$$\text{tropV} \left(\bigodot_{i=1}^m f_i^{w_i} \right) = \bigcup_{i=1}^m \text{tropV}(f_i), \text{ for } w_i > 0.$$

Proof. Let $f_i = \bigoplus_{\alpha \in A_i} c_\alpha \odot \mathbf{x}^\alpha$, $A_i \subset \mathbb{R}_{>0}^n$. If the maximum in f_j is achieved twice by \mathbf{x} , then $f_j^{w_j}(\mathbf{x}) = w_j(c_{\alpha_1} + \alpha_1 \cdot \mathbf{x}) = w_j(c_{\alpha_2} + \alpha_2 \cdot \mathbf{x})$ for some $\alpha_1 \neq \alpha_2 \in A_j$. It follows that the maximum in $\bigodot_{i=1}^m f_i^{w_i}$ is also achieved at least twice:

$$\bigodot_{i=1}^m f_i^{w_i} = w_j(c_{\alpha_1} + \alpha_1 \cdot \mathbf{x}) + \sum_{i \neq j} f_i^{w_i}(\mathbf{x}) = w_j(c_{\alpha_2} + \alpha_2 \cdot \mathbf{x}) + \sum_{i \neq j} f_i^{w_i}(\mathbf{x}).$$

On the other hand, if the maximum is achieved twice in $\bigodot_{i=1}^m f_i^{w_i}$ at \mathbf{x} , then we must be able to write the maximum as two distinct sums: $\sum_{i=1}^m w_i(c_{\alpha_i^1} + \alpha_i^1 \cdot \mathbf{x}) = \sum_{i=1}^m w_i(c_{\alpha_i^2} + \alpha_i^2 \cdot \mathbf{x})$, where $\alpha_i^1, \alpha_i^2 \in A_i$. It follows that for some j , $\alpha_j^1 \neq \alpha_j^2$, so the maximum in $f_j^{w_j}$ is achieved at least twice. \square

A tropical hypersurface is a polyhedral complex, and it can be understood combinatorially in terms of the Newton polytope of f , defined below.

Definition 4.9 (Newton polytope). Suppose $f(\mathbf{x}) = \bigoplus_{\mathbf{a} \in A} c_{\mathbf{a}} \odot \mathbf{x}^{\mathbf{a}}$ is a multivariate polynomial for some finite $A \subset \mathbb{R}^n$ and $c_{\mathbf{a}} \in \mathbb{R}$. The *support* of $f(\mathbf{x})$ is the set, denoted $\text{supp}(f)$, containing all $\mathbf{a} \in A$ such that $c_{\mathbf{a}} \neq -\infty$. The *Newton polytope* $\text{Newt}(f)$ of the polynomial $f(\mathbf{x})$ is the convex hull of its support, i.e. $\text{Newt}(f) = \text{conv}(\text{supp}(f))$. If f, g are polynomials, then $\text{Newt}(fg) = \text{Newt}(f) + \text{Newt}(g)$.

Proposition 4.10 ([24, Proposition 3.1.6]). Given a tropical signomial $f = \sum_i c_i x^{\alpha_i}$, let \underline{N}_f denote the regular subdivision of $\text{Newt}(f)$ induced by the weighting $w(\alpha_i) = c_i$. Then $\text{tropV}(f)$ is the codimension-1 skeleton of the normal complex of \underline{N}_f .

Remark. First, although Proposition 3.1.6 in [24] is originally stated for tropical polynomials, the arguments clearly hold for tropical signomials as well. Moreover, the proof in [24] shows that the subdifferential of a linear piece of f consists of the points in the corresponding cell of \underline{N} .

Definition 4.11. Given a tropical polynomial f , let \underline{N} be the regular subdivision of $\text{Newt}(f)$ induced by the coefficients of f . The *normal complex* of f is normal complex of \underline{N} ; it is a subdivision of \mathbb{R}^n .

Example 4.12. The following is an example of 4.10. Let

$$f = x^2 \oplus 4 \odot xy \oplus 3 \odot xz \oplus y^2 \oplus 4 \odot yz \oplus 3 \odot z^2. \quad (4.3)$$

4.2 depicts $\text{tropV}(f)$, the subdivision of the Newton polytope dual to it, and the lift of the Newton polytope that induces that subdivision.

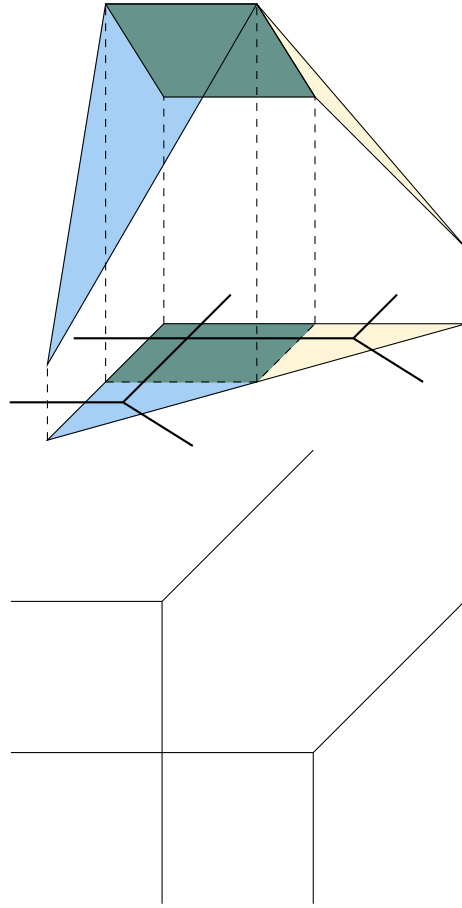


Figure 4.2: Left: A lift of $2\Delta^2 = \text{Newt}(f)$ with weights given by the coefficients of f , overlaid with $\text{tropV}(f)$ in black; right: $\text{tropV}(f)$.

Lemma 4.13. The minimum of a max-plus tropical polynomial is achieved on the cell dual to the cell of the Newton polytope containing $\bar{\mathbf{0}}$.

Proof. Let $f = \sum_i c_i x^{\alpha_i}$ be a max-plus tropical polynomial (so f is a piecewise linear convex function). Let \underline{N} be the regular subdivision of $\text{Newt}(f)$ induced by the weighting $w(\alpha_i) = c_i$. Let L be a linear piece of f , and let N_L be the cell dual to it in \underline{N} . If $\bar{\mathbf{0}} \in N_L$, then by 4.10 $\bar{\mathbf{0}}$ is in the subdifferential of f at any point in L . It then follows from 4.5 that the minimum of f is

achieved on L . □

4.1.2 Fermat-Weber problems

A Fermat-Weber problem is a geometric problem seeking the median of a collection of data points $V = \{\mathbf{v}_1, \dots, \mathbf{v}_m\} \subset X$, where X is a metric space with distance $d(\mathbf{x}, \mathbf{y})$. We are particularly interested in the Fermat-Weber points for a collection of data points in $\mathbb{R}^n/\mathbb{R}\mathbb{1}$, where the points could represent phylogenetic trees. The goal of this section is to introduce the Fermat-Weber problem, and reframe a tropical version as a problem on Newton polytopes.

In general, the median of a collection of points is not unique and hence we seek the set of all such medians, called the called *Fermat-Weber set*. The medians belonging to the Fermat-Weber set are called *Fermat-Weber points*. Formally, the Fermat-Weber points are the points $\mathbf{x} \in X$ minimizing the sum in (4.4).

Definition 4.14. The *Fermat-Weber points* on the data $V = \{\mathbf{v}_1, \dots, \mathbf{v}_m\} \subset X$ are the points $\mathbf{x} \in X$ minimizing the following sum

$$\text{FW}(V) := \frac{1}{m} \sum_{i=1}^m d(\mathbf{x}, \mathbf{v}_i). \quad (4.4)$$

In this paper, we are interested in a variant of the Fermat-Weber problem, called the *weighted Fermat-Weber problem*. This new problem seeks the points \mathbf{x} minimizing the sum in 4.5, where the weights w_i are positive real numbers.

$$\text{FW}(V, \mathbf{w}) := \frac{1}{m} \sum_{i=1}^m w_i d(\mathbf{x}, \mathbf{v}_i). \quad (4.5)$$

We will use the asymmetric tropical distance first defined by Comăneci and Joswig in [5].

Definition 4.15. The asymmetric tropical distance, $d_\Delta(\mathbf{x}, \mathbf{y})$ is:

$$d_\Delta(\mathbf{x}, \mathbf{y}) := n \max_{i \in [n]}(x_i - y_i) + \sum_{i \in [n]}(y_i - x_i). \quad (4.6)$$

When the points $\mathbf{x}, \mathbf{y} \in \mathbb{R}^n/\mathbb{R}\mathbf{1}$ are given by their unique representative in H_0 (the subspace where the coordinates sum to zero), the metric $d_\Delta(\mathbf{x}, \mathbf{y})$ can be simplified to the following

$$d_\Delta(\mathbf{x}, \mathbf{y}) := n \max_{i \in [n]}(x_i - y_i), \quad \mathbf{x}, \mathbf{y} \in H_0. \quad (4.7)$$

Note that $d_\Delta(x, y)$ is invariant under independent scalar multiplication of the input vectors, so it is well-defined on $\mathbb{R}^n/\mathbb{R}\mathbf{1}$. From now on, we will assume that all points in $\mathbb{R}^n/\mathbb{R}\mathbf{1}$ are given by their representative in H_0 . With this assumption, the distance to a point v_i can be reinterpreted as a power of a tropical linear equations, and the sum in equation 4.5 can be realized as a tropical product of tropical linear functions (possibly with real exponents).

The distance to a point v_i , denote by $f_{v_i}(\mathbf{x})$ is

$$f_{v_i}^n(\mathbf{x}) := d_\Delta(x, v_i) = n \max_j(x_j - v_{ij}) = \left(\bigoplus_{j=1}^n -v_{ij} \odot x_j \right)^n. \quad (4.8)$$

It follows that the sum in (4.5) for $d = d_\Delta$ is

$$\frac{1}{m} \sum_{i=1}^m w_i d_{\Delta}(\mathbf{x}, \mathbf{v}_i) = \frac{1}{m} \sum_{i=1}^m w_i f_{v_i}^{nw_i}(\mathbf{x}) = \frac{n}{m} \bigodot_{i=1}^m f_{v_i}^{w_i}. \quad (4.9)$$

Definition 4.16. We define *the tropical signomial associated to data V with weights \mathbf{w}* , $f_{V,\mathbf{w}}$, to be the following tropical function:

$$f_{V,\mathbf{w}}(\mathbf{x}) := \bigodot_{i=1}^m f_{v_i}^{w_i} = \bigodot_{i=1}^m \left(\bigoplus_{j=1}^n -v_{ij} \odot x_j \right)^{w_i}.$$

The tropical hypersurface $\text{tropV}(f_{v_i})$ is a tropical hyperplane centered at v_i ; it is the codimension-1 skeleton of the normal fan of the standard simplex Δ^{n-1} . By 4.8, the hypersurface $\text{tropV}(f_{V,\mathbf{w}})$ is the union of tropical hyperplanes centered at the data points v_i . The Newton polytope of $f_{V,\mathbf{w}} = \bigodot_{i=1}^m f_{v_i}^{w_i}$ is $\sum_{i=1}^m w_i \cdot \Delta^{n-1}$.

Example 4.17. The polynomial $f_{V,\mathbf{w}}(\mathbf{x})$ with $\mathbf{x} \in \mathbb{R}^3/\mathbb{R}\mathbf{1}$ and $\mathbf{w} \in \mathbb{R}^2$ has nine terms for generic V and \mathbf{w} .

$$\begin{aligned} f_{V,\mathbf{w}} &= (-v_{11} \odot x_1 \oplus -v_{12} \odot x_2 \oplus -v_{13} \odot x_3)^{w_1} \odot (-v_{21} \odot x_1 \oplus -v_{22} \odot x_2 \oplus -v_{23} \odot x_3)^{w_2} \\ &= (-v_{11} \odot -v_{21}) \odot x_1^{w_1+w_2} \oplus (-v_{11} \odot -v_{22}) \odot x_1^{w_1} x_2^{w_2} \oplus (-v_{11} \odot -v_{23}) \odot x_1^{w_1} x_3^{w_2} \\ &\oplus (-v_{12} \odot -v_{21}) \odot x_1^{w_2} x_2^{w_1} \oplus (-v_{12} \odot -v_{22}) \odot x_2^{w_1+w_2} \oplus (-v_{12} \odot -v_{23}) \odot x_2^{w_1} x_3^{w_2} \\ &\oplus (-v_{13} \odot -v_{21}) \odot x_1^{w_2} x_3^{w_1} \oplus (-v_{13} \odot -v_{22}) \odot x_2^{w_2} x_3^{w_1} \oplus (-v_{13} \odot -v_{23}) \odot x_3^{w_1+w_2}. \end{aligned}$$

Its Newton polytope is $(w_1 + w_2) \cdot \Delta^2$, and it is depicted in the lower right of 4.3, with $w_2 > w_1$. The image on the lower left of 4.3 is the Newton polytope in the special case where $w_1 = w_2 = 1$.

We now apply the results of the previous subsection to translate the

problem of optimizing $f_{V,\mathbf{w}}$ into a problem on $\text{Newt}(f_{V,\mathbf{w}})$. Since $f_{V,\mathbf{w}}$ is a function from $\mathbb{1}^\perp$ rather than \mathbb{R}^n , we need the following result to apply the results of the previous subsection.

Proposition 4.18. Given a max-plus tropical polynomial $f : \mathbb{1}^\perp \rightarrow \mathbb{R}$, let \underline{N} be the subdivision of $\text{Newt}(f)$ induced by the coefficients of f . The minimum of f is achieved on the cell dual to the cell of the Newton polytope containing $\lambda \mathbb{1}$ for any $\lambda \in \mathbb{R} \setminus \{0\}$.

Proof. Consider the following isomorphism $\mathbb{R}^n / \mathbb{R} \mathbb{1} \cong \mathbb{1}^\perp$.

$$\psi(x_1, \dots, x_{n-1}) = \left(x_1, \dots, x_{n-1}, -\sum_{i=1}^{n-1} x_i \right) \quad (4.10)$$

The Newton polytope of f lives in $(\mathbb{1}^\perp)^*$. The dual function of ψ is below.

$$\psi^*(x_1, \dots, x_n) = (x_1 - x_n, \dots, x_{n-1} - x_n) \quad (4.11)$$

Then $\psi^*(\lambda \mathbb{1}) = \lambda(1 - 1, \dots, 1 - 1) = \bar{\mathbf{0}}$. 4.5 says that for a tropical function $g : \mathbb{R}^n \rightarrow \mathbb{R}$, the linear piece of g whose dual cell contains $\bar{\mathbf{0}}$ is the linear piece achieving the minimum. Combining this result with the map ψ , it follows that $f : \mathbb{1}^\perp \rightarrow \mathbb{R}$ achieves its minimum on the linear piece dual to the cell containing $\lambda \mathbb{1}_n$. \square

4.1.3 Tropical convexity

Tropical Factorization

Let $f = \odot_{i=1}^m f_i$ be a tropical signomial that factors into a product of tropical signomials. The following theorem tells us how to compute the tropical hypersurface $\text{tropV}(f)$ in terms of a subdivision of the Cayley polytope. Let $P_i = \text{Newt}(f_i)$, $P = \sum_i P_i$, and write $f_i = \sum c_{i,\alpha} \mathbf{x}^\alpha$.

Theorem 4.19 (Corollary 4.9 in [23]). Let \underline{C} be the regular subdivision of $\text{Cayley}(P_1, \dots, P_m)$ induced by the weights $w(e_i, \alpha) = c_{i,\alpha}$. Then the mixed subdivision of P corresponding to \underline{C} coincides with the regular subdivision of P induced by the coefficients of f .

Recall that in the weighted tropical Fermat-Weber problem, $f_{V,\mathbf{w}}$ factors into linear pieces, and so 4.19 applies.

Corollary 4.20. Let \underline{N} be the subdivision of $\text{Newt}(f_{V,\mathbf{w}})$ induced by the coefficients of $f_{V,\mathbf{w}}$. Then $\underline{N} = \underline{C} \cap \{\frac{1}{m} \mathbb{1}_m\} \times \mathbb{R}^n$. In particular, the cell of \underline{N} containing $\lambda \mathbb{1}_n$ corresponds to the cell of \underline{C} containing $(\frac{1}{m} \mathbb{1}_m, \frac{|\mathbf{w}|}{mn} \mathbb{1}_n)$.

Proof. The point $(\frac{1}{m} \mathbb{1}_m, \frac{|\mathbf{w}|}{mn} \mathbb{1}_n)$ is the barycenter of $\text{Cayley}(P_1, \dots, P_m)$, so in particular, it lies in $\text{Cayley}(P_1, \dots, P_m) \cap \{\frac{1}{m} \mathbb{1}_m\} \times \mathbb{R}^n$. Apply 4.19 and then 2.14. \square

Proposition 4.21. Let $P_i = \text{Newt}(f_{v_i})$, and let \underline{C}' be the subdivision of $\text{Cayley}(P_1, \dots, P_m)$ induced by $w(\alpha_j, e_i) = -v_{ij}$. Then the subdivision of $P_{\mathbf{w}} = \sum_{i=1}^m w_i P_i$ induced by the coefficients of $f_{V,\mathbf{w}}$ is $\underline{C}' \cap \{\mathbf{w}\} \times \mathbb{R}^n$. In particular, the cell of \underline{P} containing $\mathbb{1}_n$ corresponds to the cell of \underline{C}' containing $(\mathbf{w}, \frac{1}{n} \mathbb{1}_n)$.

Proof. Apply 2.15 to 4.20. □

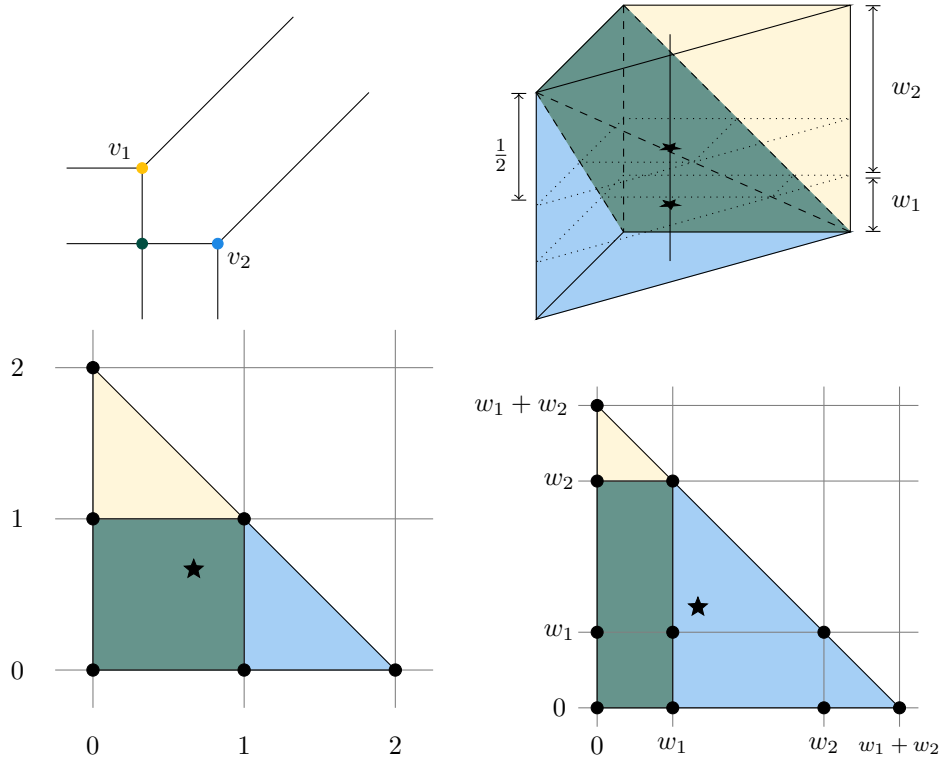


Figure 4.3: Subdivisions with weightings. Clockwise starting on top left: Two tropical hyperplanes in $\mathbb{T}\mathbb{R}^2$, the corresponding regular subdivision of $\Delta^1 \times \Delta^2$, the corresponding mixed subdivision of $(w_1 + w_2)\Delta^2$ (weighted FW problem), and the corresponding mixed subdivision of $2\Delta^2$ (unweighted FW problem).

Tropical Convex Hull

Definition 4.22. The *min-tropical convex hull* of a set of points $A \subset \mathbb{R}^n / \mathbb{R}\mathbb{1}$, denoted $\text{tconv}^{\min}(A)$ or just $\text{tconv}(A)$, is the set of all tropical linear combi-

nations of points in A , that is,

$$\mathbf{tconv}(A) := \{\lambda_1 \odot \mathbf{a}_1 \oplus_{\min} \cdots \oplus_{\min} \lambda_k \odot \mathbf{a}_k \mid \lambda_i \in \mathbb{R}, \mathbf{a}_i \in A, k \in \mathbb{Z}_{>0}\}. \quad (4.12)$$

If A is a finite set, then $\mathbf{tconv}(A)$ is called a *tropical polytope*.

Note that the tropical convex hull is independent of the representatives in $\mathbb{R}^n/\mathbb{R}\mathbb{1}$ we choose for the points in A . That is, if $\mathbf{v}'_i = \alpha_i \odot \mathbf{v}_i$, $\lambda_i \in \mathbb{R}$, then with $\lambda'_i = \lambda_i - \alpha_i$

$$\lambda_1 \odot v_1 \oplus \cdots \oplus \lambda_m \odot v_m = (\lambda_1 - \alpha_1) \odot v'_1 \oplus \cdots \oplus (\lambda_m - \alpha_m) \odot v_m = \lambda'_1 \odot v'_1 \oplus \cdots \oplus \lambda'_m \odot v'_m.$$

Example 4.23. Let $v_1 = (0, 0, 0)$, and $v_2 = (1, -1, 0)$. The tropical polytope $\mathbf{tconv}(v_1, v_2)$ consists of points of the form $\lambda_1 \odot v_1 \oplus \lambda_2 \odot v_2$, and is illustrated in 4.4. The tropical polytope consists of three points, connected by two classical line segments.

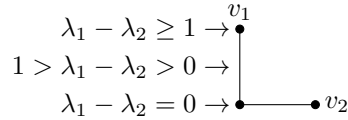


Figure 4.4: The tropical line segment between $v_1 = (0, 0, 0)$ and $v_2 = (1, -1, 0)$.

It turns out that the tropical convex hull of the data points coincides with the bounded part of the tropical hypersurface $\mathbf{tropV}(f_V)$.

Theorem 4.24 (Theorem 5.2.11 in [24]). The bounded part of the tropical hypersurface f_V is $\mathbf{tconv}^{\min}(v_1, \dots, v_m)$.

We now see that f_V and $f_{V,\mathbf{w}}$ define the same tropical hypersurface. Thus, the bounded part $\text{tropV}(f_{V,\mathbf{w}})$ is the tropical convex hull of the v_i 's.

Lemma 4.25. For any $\mathbf{w} \in \mathbb{R}^m$, $\text{tropV}(f_V) = \text{tropV}(f_{V,\mathbf{w}})$.

Proof. By 4.8, $\text{tropV}(f_v^w) = \text{tropV}(f_v)$ for any $v \in \mathbb{1}^\perp$, and any $w > 0$. Applying 4.8 to f_V and $f_{V,\mathbf{w}}$, it follows that

$$\text{tropV}(f_V) = \bigcup_{i=1}^m \text{tropV}(f_{v_i}) = \text{tropV}(f_{V,\mathbf{w}}).$$

□

Corollary 4.26. The bounded part of the tropical hypersurface $f_{V,\mathbf{w}}$ is $\text{tconv}^{\min}(v_1, \dots, v_m)$.

4.2 Solving the Weighted Tropical Fermat-Weber Problem

In this section, we use combinatorics and tropical geometry to solve the weighted Fermat-Weber problem for $\mathbb{R}^n/\mathbb{R}\mathbb{1}$ equipped with the tropical asymmetric distance. We begin by discussing the extrema of tropical polynomials.

4.2.1 Containment of weighted Fermat-Weber points

Theorem 4.27. Given data points $v_1, \dots, v_m \in \mathbb{R}^n/\mathbb{R}\mathbb{1}$, and positive weights w_1, \dots, w_m , the weighted Fermat-Weber points under the tropical asymmetric metric are a cell of $\text{tconv}(v_1, \dots, v_m)$.

Proof. According to 4.26, $\text{tconv}(v_1, \dots, v_m)$ is the bounded part of $\text{tropV}(f_{V, \mathbf{w}})$. The bounded cells of $\text{tropV}(f_{V, \mathbf{w}})$ are exactly those cells dual to interior cells of the Newton polytope, so by 4.18, it suffices to show that $\lambda \mathbb{1}$ is in the interior of $\text{Newt}(f_{V, \mathbf{w}})$. The vertices of $\text{Newt}(f_{V, \mathbf{w}})$ are $|\mathbf{w}|e_i$, and their average, $\frac{|\mathbf{w}|}{n} \mathbb{1}$, is in the interior of the Newton polytope. This proves the Fermat-Weber points are achieved on a bounded cell of $\text{tropV}(f_{V, \mathbf{w}})$, and therefore form a cell of $\text{tconv}(v_1, \dots, v_m)$. \square

4.2.2 Any cell can be the weighted Fermat-Weber cell

The following result shows that we can pick weights w_i so that the weighted barycenter lies in any interior cell of the subdivision of the Cayley polytope. This finishes the proof of the main theorem.

Theorem 4.28. Given some data points $\mathbf{v}_1, \dots, \mathbf{v}_m \in \mathbb{R}^n / \mathbb{R} \mathbb{1}$, and any simplex S in $\Delta^{r-1} \times \Delta^{n-1}$, which intersects the relative interior of $\Delta^{r-1} \times \Delta^{n-1}$, there is a choice of weights $w_1, \dots, w_m \in [0, 1]$ with $\sum w_i = 1$, so that S contains the point $(w_1, \dots, w_m, \frac{1}{n} \mathbb{1}_n)$.

The proof uses a well-known correspondence between subsets of the vertices of $\Delta^{m-1} \times \Delta^{n-1}$ and subgraphs of $K_{m,n}$ (the complete bipartite graph with m left vertices, and n right vertices), which we now briefly recall (see [10, §6.2.2] for more details). The vertex (e_i, e_j) in a simplex $S \subseteq \Delta^{r-1} \times \Delta^{n-1}$ corresponds to the edge between left vertex i and right vertex j in the bipartite graph. Thus, a subset of vertices $A \subseteq \Delta^{r-1} \times \Delta^{n-1}$ corresponds to the subgraph of $K_{m,n}$.

Example 4.29 (Simplex-Forest Correspondence for $m = n = 2$). The prod-

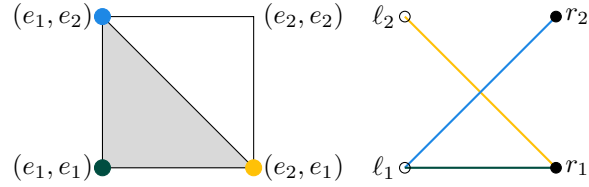


Figure 4.5: Vertices in the product of simplices (left) correspond to the color-coded edges of the bipartite graph (right).

product of two 2-simplices (i.e. line segments) is a square; the corresponding bipartite graph has two left vertices and two right vertices. Both are illustrated in 4.5. The vertex (e_i, e_j) in the simplex corresponds to the edge (l_i, r_j) in the bipartite graph. For example, the top left vertex of the shaded gray simplex, (e_1, e_2) , corresponds to the edge (l_1, r_2) . The shaded simplex is full-dimensional, so it corresponds to a spanning tree of $K_{2,2}$ (see 4.30).

Lemma 4.30 (Lemma 6.2.8 in [10]). Let A be a subset of the vertices of $\Delta^{m-1} \times \Delta^{n-1}$. Then,

1. $\text{conv}(A)$ is a simplex if and only if the corresponding subgraph of $K_{m,n}$ is a forest.
2. $\text{conv}(A)$ is full dimensional if and only if the corresponding subgraph of $K_{m,n}$ is spanning and connected.

Proof of 4.28. Let S be a simplex in $\Delta^{r-1} \times \Delta^{n-1}$, and let F be the corresponding forest in $K_{r,n}$. Assume that $S \cap \text{int}(\Delta^{r-1} \times \Delta^{n-1}) \neq \emptyset$ (so F is a spanning forest).

A point $(\mathbf{p}, \mathbf{q}) \in \mathbb{R}^m \times \mathbb{R}^n$ lies in S if it can be written as a convex combination of the vertices of S . In terms of the forest F , (\mathbf{p}, \mathbf{q}) lies in S if there exist $\lambda(e) > 0$ for each edge $e \in E(F)$ such that the sum of edge

weights on any left vertex adds up to the corresponding \mathbf{p} coordinate, and the sum of edge weights on any right vertex adds up to the corresponding \mathbf{q} coordinate. Let $r(e)$ be the node on the right side connected to e , and let $\ell(e)$ be the node on the left side connected to e . The choice of λ 's in (4.13) leads to a valid choice of weights w_1, \dots, w_m (given in (4.14)) so that S contains the weighted barycenter.

$$\lambda(e) := \frac{1}{n \cdot \deg r(e)}. \quad (4.13)$$

$$w_i := \sum_{e \text{ s.t. } \ell(e)=i} \lambda(e). \quad (4.14)$$

The equations in (4.15) show that the weights on any right node sum to $\frac{1}{n}$ (since F is spanning, every vertex has at least one edge); by definition, the weights on the i th left node sum to w_i . It follows that $\mathbf{b} = (w_1, \dots, w_m, \frac{1}{n} \mathbb{1})$ lies in the relative interior of S .

$$\sum_{r(e)=j} \frac{1}{n \cdot \deg(j)} = \frac{1}{n} \sum_{r(e)=j} \frac{1}{\deg(j)} = \frac{1}{n} \deg(j) \frac{1}{\deg(j)} = \frac{1}{n}. \quad (4.15)$$

Moreover, w_1, \dots, w_m is a valid choice of weights for the Fermat-Weber problem. The weights w_i are positive because F is spanning, so the sum in (4.14) is never empty; The equations in (4.16) show that the w_i sum to one.

$$\sum_{i=1}^m w_i = \sum_e \lambda(e) = \sum_{j=1}^n \sum_{r(e)=j} \frac{1}{n \cdot \deg(j)} = \sum_{j=1}^n \frac{1}{n} \sum_{r(e)=j} \frac{1}{\deg(j)} = \sum_{j=1}^n \frac{1}{n} = n \frac{1}{n} = 1. \quad \square \quad (4.16)$$

Corollary 4.31. Given a cell T in the tropical polytope $\text{tconv}(\mathbf{v}_1, \dots, \mathbf{v}_m)$,

there is a choice of weights w_1, \dots, w_m so that T is the set of weighted tropical Fermat-Weber points for $\mathbf{v}_1, \dots, \mathbf{v}_m$ with weights w_1, \dots, w_m .

Chapter 5

Singular Locus of Linear Structural Equation Models

This chapter contains ongoing work with Dr. Elizabeth Gross and Dr. Nicolette Meshkat.

5.1 Introduction

In this section we are motivated by identifying model parameters for linear structural equation models. This gives a more detailed understanding of identifiability issues that can arise. In this setting unidentifiable parameters are encoded as singularities of varieties colloquially known as the locus of non-identifiable parameters, which in short, we will call the singular locus. This is motivation for the following definition.

Definition 5.1. Let $V \subset \mathbb{K}^n$ be the image of a polynomial map $\phi : \mathbb{R}^m \rightarrow \mathbb{R}^n$ with $\phi_i(\mathbf{x}) = f_i(\mathbf{x})$. The *Jacobian* $J(\mathbf{x})$ of the map ϕ is the $n \times m$ matrix

with entries

$$J_{(i,j)} = \frac{\partial}{\partial x_j} f_i(\mathbf{x}).$$

A point $\mathbf{x} \in \mathbb{R}^n$ is called a *singular* of ϕ if $J(\mathbf{x})$ has rank less than $n - d$, where d is the dimension of V . The *singular locus* of ϕ is the set of all singular points of ϕ . The *singular locus ideal* of ϕ is the ideal $I \subset \mathbb{R}[\lambda, \omega]$ defining the singular locus.

We end this brief introduction by introducing language for the terms in the trek rule (Equation 2.4). Recall that any trek $\tau = (P, P')$ between i and j is a path of the form

$$\begin{cases} i \leftarrow i_k \leftarrow \cdots \leftarrow i_0 \longrightarrow \cdots \rightarrow j_\ell \rightarrow j, & \text{or} \\ i \leftarrow i_k \leftarrow \cdots \leftarrow i_0 \leftrightarrow j_0 \rightarrow \cdots j_\ell \rightarrow j \end{cases}$$

We will denote by $w(\tau)$ the *trek monomial* corresponding to $\tau = (P, P')$, given by

$$w(\tau) = \text{peak}(P, P') \lambda^P \lambda^{P'}.$$

5.2 Singular Locus Formulas

In this section we describe the set of non-identifiable parameters as the solutions of a set of polynomial equations in λ and ω . We compute the singular locus ideal for linear structural equation models given by directed star graphs with inward and outward arrows. In this setting, the singular locus ideal is the ideal of certain minors of the Jacobian of the covariance parameteriza-

tion map ϕ_G . Motivated by simplifying these determinant calculations, we later prove a result that gives a description of the entries of a row reduced Jacobian for models given by disjoint directed paths.

Theorem 5.2. The singular locus ideal for the star on n nodes with inward arrows is generated by a single monomial, the product of the ω corresponding to the leaf vertices.

Proof. Consider a star with n nodes labeled $1, \dots, n$ where n is the central node and each edge points inward toward n . The entries of the matrix $\Sigma = \phi_G$ are

$$\sigma_{ij} = \begin{cases} \omega_{ii} & \text{if } i = j < n \\ \omega_{ii}\lambda_{in} & \text{if } i < j = n \\ \omega_{nn} + \sum_{k=1}^{n-1} \omega_{kk}\lambda_{kn}^2 & \text{if } i = j = n \\ 0 & \text{otherwise.} \end{cases}$$

In this proof, we will refer to the Jacobian as the transpose of the Jacobian in Definition 5.1. The Jacobian of Σ will have a column of zeros whenever σ_{ij} is zero; there are $(n-1)(n-2)/2$ of them. Thus, the Jacobian matrix has

$$\begin{aligned} n + \frac{n(n-1)}{2} - \frac{(n-1)(n-2)}{2} &= n + \frac{1}{2}(n^2 - n - n^2 + 3n - 2) \\ &= n + \frac{1}{2}(2n - 2) \\ &= n + (n - 1) \end{aligned}$$

nonzero columns. Since the expected dimension of the image of ϕ_G is the number of vertices plus the number of edges, then the number of nonzero

columns of the Jacobian is equal to the expected dimension. Therefore, the singular locus ideal is the determinant of the submatrix obtained by deleting the columns of zeros of the Jacobian matrix. We claim that this submatrix has determinant $\prod_{i=1}^{n-1} \omega_{ii}$.

Notice that the first $n - 1$ unit vectors are columns of this submatrix, namely the gradients of the entries $\sigma_{ii} = \omega_{ii}$ for all $i < n$. By consecutively using an expansion by minors along these unit columns, we see that the determinant is completely dependent on an even smaller submatrix of the Jacobian matrix. We can organize the columns of this submatrix by $\{\sigma_n n, \sigma\}$ according to the below diagram, where, for instance, the $(\lambda_{1n}, \sigma_{2n})$ -entry is $\frac{\partial}{\partial \lambda_{1n}}(\sigma_{2n})$.

$$\begin{array}{c} \omega_{nn} \\ \lambda_{1n} \\ \vdots \\ \lambda_{n-1,n} \end{array} \begin{pmatrix} \sigma_{nn} & \sigma_{1n} & \cdots & \sigma_{n-1,n} \\ & & & \\ & & & \\ & & & \\ & & & \end{pmatrix}$$

A direct calculation shows the above matrix is lower triangular and has diagonal entries $1, \omega_{11}, \dots, \omega_{n-1,n-1}$. Indeed, the above matrix is lower triangular since

$$\frac{\partial}{\partial \omega_{nn}}(\sigma_{in}) = \frac{\partial}{\partial \omega_{nn}}(\omega_{ii} \lambda_{in}) = 0$$

for all $i = 1, \dots, n - 1$, and

$$\frac{\partial}{\partial \lambda_{in}}(\sigma_{jn}) = \frac{\partial}{\partial \lambda_{in}}(\omega_{jj} \lambda_{jn}) = 0$$

for all $i < j < n$. Moreover, the diagonal entries are

$$\frac{\partial}{\partial \omega_{nn}}(\sigma_{nn}) = \frac{\partial}{\partial \omega_{nn}}(\omega_{nn} + \sum_{k=1}^{n-1} \omega_{kk} \lambda_{kn}^2) = 1$$

and, for $i = 1, \dots, n-1$,

$$\frac{\partial}{\partial \lambda_{in}}(\sigma_{in}) = \frac{\partial}{\partial \lambda_{in}}(\omega_{ii} \lambda_{in}) = \omega_{ii}.$$

The result follows since the determinant of a lower triangular matrix is the product of its diagonal entries. \square

Theorem 5.3. The singular locus ideal for a star on n nodes with outward arrows is generated by the monomial ω_{nn}^{n-1} where the central node is labeled n .

Proof. Consider a star with n nodes labeled $1, \dots, n$ where n is the label for the central node and each edge points outward, away from n . The entries of the matrix Σ are

$$\sigma_{ij} = \begin{cases} \omega_{ii} + \omega_{nn} \lambda_{ni}^2 & \text{if } i = j < n \\ \omega_{nn} \lambda_{ni} \lambda_{nj} & \text{if } i \neq j < n \\ \omega_{nn} \lambda_{ni} & \text{if } i \neq j = n \\ \omega_{nn} & \text{otherwise,} \end{cases}$$

The expected dimension of the image of this matrix is $d = n + (n-1)$, the number of vertices and edges of the star. Again, in this proof we shall refer to the Jacobian as the transpose of the matrix in Definition 5.1. We

claim that one of the $d \times d$ minors of the Jacobian J of Σ is equal to ω_{nn}^{n-1} and that all remaining non-zero $d \times d$ minors of the Jacobian J are multiples of ω_{nn}^{n-1} , and hence, the singular locus is the ideal generated by this monomial. By an elementary calculus computation, observe that the Jacobian J has the following form:

$$\begin{array}{c} \sigma_{ii} \quad \sigma_{nn} \quad \sigma_{jk} \quad \sigma_{in} \\ \omega_{ii} \left(\begin{array}{cccc} I & 0 & 0 & 0 \\ v_1 & 1 & v_2 & v_3 \\ A & 0 & (\omega_{nn}I)B & \omega_{nn}I \end{array} \right) \\ \lambda_{in} \end{array}$$

where i ranges from $1, \dots, n-1$, j and k satisfy $1 \leq j < k < n$, and I denotes the $(n-1) \times (n-1)$ identity matrix.

Indeed the monomial ω_{nn}^{n-1} belongs to the singular locus ideal. The minor of J which gives rise to this monomial is the determinant of the submatrix obtained by taking the columns indexed by $\{\sigma_{ii}, \sigma_{jn}\}_{j \in [n-1]}^{i \in [n]}$. The row of this submatrix indexed by ω_{ii} for $i = 1, \dots, n-1$ is the i th standard unit vector. Moreover, the column indexed by σ_{nn} is the n th standard unit vector. By consecutively using an expansion by minors along these unit rows followed by an expansion along the unit column, we see that we need only compute the determinant of the submatrix indexed by rows $\{\lambda_{n1}, \dots, \lambda_{n,n-1}\}$ and columns $\{\sigma_{1n}, \dots, \sigma_{n-1,n}\}$. This $(n-1) \times (n-1)$ submatrix is a diagonal matrix since

$$\frac{\partial}{\partial \lambda_{ni}}(\sigma_{jn}) = \frac{\partial}{\partial \lambda_{ni}}(\omega_{nn} \lambda_{nj}) = 0$$

for $i \neq j$. Moreover, the diagonal entries are

$$\frac{\partial}{\partial \lambda_{ni}}(\sigma_{in}) = \frac{\partial}{\partial \lambda_{ni}}(\omega_{nn}\lambda_{ni}) = \omega_{nn},$$

so the determinant is ω_{nn}^{n-1} . All that is left to show is that the remaining minors are multiples of ω_{nn}^{n-1} .

For the remaining minors, we must compute the determinant of the submatrix of J by choosing $d = n + (n-1)$ columns. Note that for $i = 1, \dots, n-1$, if any one of the columns σ_{ii} is not present in this submatrix, then the ω_{ii} row is the zero vector. Hence, the corresponding minor is zero. Thus, assume that the columns σ_{ii} for $i = 1, \dots, n-1$ are present in this submatrix. After the appropriate expansion by minors, we see that we need only compute the $n \times n$ minors of the submatrix, say \hat{J} , of J after removing the rows ω_{ii} and columns σ_{ii} for $i = 1, \dots, n-1$. Observe that \hat{J} can be factored so that one of the factors is the matrix

$$\begin{pmatrix} 1 & 0 \\ 0 & \omega_{nn}I \end{pmatrix}.$$

Therefore, regardless of the choice of n columns of \hat{J} , the corresponding minor is a multiple of ω_{nn}^{n-1} since the determinant of a product of matrices is the product of determinants of the factors. \square

Example 5.4. Consider the model below consisting of two disjoint paths.

$$\begin{array}{ccccccc} 1 & \longrightarrow & 2 & \longrightarrow & 3 & & \\ & & & & & & \\ 4 & \longrightarrow & 5 & & & & \end{array}$$

The associated Jacobian of the model is

$$\begin{array}{c}
 \omega_{11} \quad \omega_{22} \quad \omega_{33} \quad \omega_{44} \quad \omega_{55} \quad \lambda_{12} \quad \lambda_{23} \quad \lambda_{45} \\
 \sigma_{11} \left(\begin{array}{cccccccc}
 1 & 0 & 0 & 0 & 0 & 0 & 0 & 0 \\
 \lambda_{12}^2 & 1 & 0 & 0 & 0 & 2\omega_{11}\lambda_{12} & 0 & 0 \\
 \lambda_{1 \rightarrow 3}^2 & \lambda_{23}^2 & 1 & 0 & 0 & 2\omega_{11}\lambda_{12}\lambda_{23}^2 & 2\omega_{11}\lambda_{12}^2\lambda_{23} + 2\omega_{22}\lambda_{23} & 0 \\
 0 & 0 & 0 & 1 & 0 & 0 & 0 & 0 \\
 0 & 0 & 0 & \lambda_{45}^2 & 1 & 0 & 0 & 2\omega_{44}\lambda_{45} \\
 \lambda_{12} & 0 & 0 & 0 & 0 & \omega_{11} & 0 & 0 \\
 \lambda_{1 \rightarrow 3} & 0 & 0 & 0 & 0 & \omega_{11}\lambda_{23} & \omega_{11}\lambda_{12} & 0 \\
 \lambda_{12}^2\lambda_{23} & \lambda_{23} & 0 & 0 & 0 & 2\omega_{11}\lambda_{1 \rightarrow 3} & \omega_{11}\lambda_{12}^2 + \omega_{22} & 0 \\
 0 & 0 & 0 & \lambda_{45} & 0 & 0 & 0 & \omega_{44}
 \end{array} \right)
 \end{array}$$

and its reduced form is

$$\begin{array}{c}
 \omega_{11} \quad \omega_{22} \quad \omega_{33} \quad \omega_{44} \quad \omega_{55} \quad \lambda_{12} \quad \lambda_{23} \quad \lambda_{45} \\
 \sigma_{11} \left(\begin{array}{cccccccc}
 1 & 0 & 0 & 0 & 0 & 0 & 0 & 0 \\
 0 & 1 & 0 & 0 & 0 & 0 & 0 & 0 \\
 0 & 0 & 1 & 0 & 0 & 0 & 0 & 0 \\
 0 & 0 & 0 & 1 & 0 & 0 & 0 & 0 \\
 0 & 0 & 0 & 0 & 1 & 0 & 0 & 0 \\
 0 & 0 & 0 & 0 & 0 & \omega_{11} & 0 & 0 \\
 0 & 0 & 0 & 0 & 0 & 0 & \omega_{11}\lambda_{12} & 0 \\
 0 & 0 & 0 & 0 & 0 & 0 & \omega_{22} & 0 \\
 0 & 0 & 0 & 0 & 0 & 0 & 0 & \omega_{44}
 \end{array} \right) .
 \end{array}$$

Lemma 5.5. Let G be an acyclic digraph without bidirected edges. If G

consists of disjoint paths, then the singular locus is monomial. Moreover, the Jacobian J can be reduced to the following matrix J^* with monomial entries

$$J_{\{i,j\},\pi}^* = \begin{cases} 1 & \text{if } i = j, \pi = \omega_{ii} \\ \omega_{ii}\lambda_{i \rightarrow k} & \text{if } i \in \mathbf{an}(j), \pi = \lambda_{kj} \\ 0 & \text{otherwise} \end{cases}$$

where $i, j \in G$ and π ranges over all ω and λ parameters.

Proof. If G is a disjoint union of paths, then the rows and columns can be partitioned based on the individual paths, specifically its submatrices corresponding to two distinct paths have disjoint rows and columns. Thus, to reduce the Jacobian J it suffices to reduce each submatrix corresponding to a single path individually. Without loss of generality let G be the single path $1 \rightarrow 2 \rightarrow \dots \rightarrow m$. Use the following row and column ordering on the Jacobian:

$$J = \begin{matrix} & \omega & \lambda \\ \begin{matrix} \sigma_{ii} \\ \sigma_{ij} \end{matrix} & \begin{pmatrix} J_{11} & J_{12} \\ J_{21} & J_{22} \end{pmatrix} \end{matrix}.$$

As in Example 5.4, the rows of J are indexed by pairs of vertices, first by pairs of the same vertex $\{i, i\}$ then followed by pairs of distinct vertices $\{i, j\}$ with $i \in \mathbf{an}(j)$ or in this case $i < j$; both sets of rows are ordered lexicographically. To show that the singular locus is monomial, first reduce the Jacobian J to the matrix described in the statement of the lemma.

For all i, j with $i < j$ and $(k, k + 1)$ an edge of the graph, we have

$$J_{\{i,j\},\omega_{pp}} = \begin{cases} \lambda_{p \rightarrow i}^2 \lambda_{i \rightarrow j} & \text{if } p \leq i \\ 0 & \text{otherwise} \end{cases}$$

$$J_{\{i,j\},\lambda_{k,k+1}} = \begin{cases} \sum_{p \leq k} 2\omega_{pp} \frac{\lambda_{p \rightarrow i}^2}{\lambda_{k,k+1}} \lambda_{i \rightarrow j} & \text{if } k < i \\ \sum_{p \leq i} \omega_{pp} \lambda_{p \rightarrow i}^2 \frac{\lambda_{i \rightarrow j}}{\lambda_{k,k+1}} & \text{if } i \leq k < j \\ 0 & \text{otherwise.} \end{cases}$$

For each i, j such that $i < j$, replace row $J_{\{i,j\}}$ with $J_{\{i,j\}} - \lambda_{i \rightarrow j} J_{\{i,i\}}$. The entries of this new row are zero except for in columns $\lambda_{k,k+1}$ with $i \leq k < j$ where the new entry is $\sum_{p \leq i} \omega_{pp} \lambda_{p \rightarrow i}^2 \frac{\lambda_{i \rightarrow j}}{\lambda_{k,k+1}}$. In particular, J_{21} has been reduced to a matrix of zeros. Next, observe J_{11} is a lower triangular matrix with diagonal entries $J_{\{i,i\},\omega_{ii}} = \lambda_{i \rightarrow i}^2 \lambda_{i \rightarrow i} = 1$. Row-reduce J_{11} to a diagonal matrix with 1's along the diagonal, the reduced matrix has the form $\begin{pmatrix} I & J_{12}^* \\ 0 & J_{22}^* \end{pmatrix}$. Since J_{21} has been reduced to a matrix of zeros, use column operations to reduce J_{12}^* to a matrix of zeros. After all these reductions, the reduced Jacobian J^* now has the form $\begin{pmatrix} I & 0 \\ 0 & J_{22}^* \end{pmatrix}$. Since J^* is block diagonal then row operations on J^* restrict to row operations on its blocks. For each i, j such that $i < j - 1$, replace row $(J_{22}^*)_{\{i,j\}}$ with $(J_{22}^*)_{\{i,j\}} - \lambda_{j-1,j} (J_{22}^*)_{\{i,j-1\}}$,

its new entries are

$$(J_{22}^*)_{\{i,j\},\lambda_{k,k+1}} = \begin{cases} \sum_{p \leq i} \omega_{pp} \lambda_{p \rightarrow i}^2 \lambda_{i \rightarrow j-1} & \text{if } k = j - 1 \\ 0 & \text{otherwise.} \end{cases}$$

Lastly, for $i = 2, \dots, m - 1$ and $j > i$, replace row $(J_{22}^*)_{\{i,j\}}$ with $(J_{22}^*)_{\{i,j\}} - \lambda_{i-1,i} (J_{22}^*)_{\{i-1,j\}}$. Then the remaining nonzero entry in row $\{i, j\}$ is

$$\sum_{p \leq i} \omega_{pp} \lambda_{p \rightarrow i}^2 \lambda_{i \rightarrow j-1} - \lambda_{i-1,i} \sum_{p \leq i-1} \omega_{pp} \lambda_{p \rightarrow i-1}^2 \lambda_{i-1 \rightarrow j-1} = \omega_{ii} \lambda_{i \rightarrow j-1}.$$

After this final row reduction, the Jacobian has been reduced to a matrix as described in the statement of the Lemma. In particular, the entries are monomial. Further, we can see that the non-zero minors are determinants of lower triangular submatrices. Hence, the nonzero minors are monomial and thus the singular locus ideal is monomial. \square

The remainder of this chapter includes an investigation of identifiability of linear structural equation models given by mixed graphs with bidirected edges. Furthermore, we discuss the relationship between identifiability and the singular locus being defined by monomials.

5.3 Bidirected edges

Proposition 5.6. Let G be a single directed path where one or more directed edges are replaced with a bidirected edge. Then the singular locus ideal of ϕ_G is monomial.

Proof. We can take the associated path model with no bidirected edges and change the directed edges to bidirected edges.

Using Lemma 5.5 the reduced Jacobian matrix of a directed path $1 \rightarrow 2 \rightarrow \dots \rightarrow n$ (and no bidirected edges) is

$$\begin{array}{c} \omega_{ii} \quad \lambda_{ij} \\ \sigma_{ii} \\ \sigma_{1k} \\ \sigma_{2k} \\ \vdots \\ \sigma_{n-1,n} \end{array} \begin{pmatrix} I & 0 \\ 0 & B_1 \\ 0 & B_2 \\ \vdots & \vdots \\ 0 & B_n \end{pmatrix}$$

where σ_{jk} indexes rows $\sigma_{j,j+1}, \dots, \sigma_{jn}$. The block matrix B_j is a $n-j$ by $n-1$ matrix whose first $j-1$ columns are zero columns and the remaining $n-j$ by $n-j$ matrix is a diagonal matrix C_j for $j = 1, \dots, n$ and $k = j+1, \dots, n$:

$$B_j = \begin{pmatrix} 0 & C_j \end{pmatrix}$$

where C_j looks like:

$$\begin{array}{c} \lambda_{j,j+1} \quad \lambda_{j+1,j+2} \quad \dots \quad \lambda_{n-1,n} \\ \sigma_{j,j+1} \\ \sigma_{j,j+2} \\ \vdots \\ \sigma_{j,n} \end{array} \begin{pmatrix} \omega_{jj} & 0 & \dots & 0 \\ 0 & \omega_{jj}\lambda_{j,j+1} & \dots & 0 \\ \vdots & \vdots & \vdots & \vdots \\ 0 & 0 & \dots & \omega_{jj}\lambda_{j \rightarrow n-1} \end{pmatrix}$$

Changing a directed edge $\lambda_{i,i+1}$ to a bidirected edge $\omega_{i,i+1}$ has the following effect on the Jacobian. Rows corresponding to treks from k to $i+1$

through rows corresponding to treks from k to n , where k is upstream of i , become zero rows in the Jacobian matrix. Furthermore, we can obtain the reduced Jacobian matrix via row reduction as in the proof of Lemma 5.5 since pairs of cancelling terms in the directed case still cancel if we change the entries of J^* via a (monomial) map which sends ω_{ii} to 1 and $\lambda_{i,i+1}$ to $\omega_{i,i+1}$.

Altogether, this has the following effect on the diagonal entries of C_j . If $i = j$, then the C_j looks like:

$$\begin{matrix} & \omega_{i,i+1} & \lambda_{i+1,i+2} & \dots & \lambda_{n-1,n} \\ \sigma_{i,i+1} & \left(\begin{array}{cccc} 1 & 0 & \dots & 0 \\ 0 & \omega_{i,i+1} & \dots & 0 \\ \vdots & \vdots & \vdots & \vdots \\ 0 & 0 & \dots & \omega_{i,i+1}\lambda_{i+1 \rightarrow n-1} \end{array} \right) \end{matrix}$$

otherwise if j is upstream of i , then C_j looks like:

$$\begin{matrix} & \lambda_{j,j+1} & \lambda_{j+1,j+2} & \dots & \lambda_{i-1,i} & \omega_{i,i+1} & \dots & \lambda_{n-1,n} \\ \sigma_{j,j+1} & \left(\begin{array}{ccccccc} \omega_{jj} & 0 & \dots & 0 & 0 & \dots & 0 \\ 0 & \omega_{jj}\lambda_{j,j+1} & \dots & 0 & 0 & \dots & 0 \\ \vdots & \vdots & \vdots & \vdots & \vdots & \vdots & \vdots \\ 0 & 0 & \dots & \omega_{jj}\lambda_{j \rightarrow i-1} & 0 & \dots & 0 \\ 0 & 0 & 0 & 0 & 0 & \dots & 0 \\ \vdots & \vdots & \vdots & \vdots & \vdots & \vdots & \vdots \\ 0 & 0 & \dots & 0 & 0 & \dots & 0 \end{array} \right) \end{matrix}$$

and finally, if j is downstream of i , then C_j is unaffected.

Since the reduced Jacobian matrix still has monomial entries, and it is still full rank due to the Brito and Pearl result [1], then the singular locus will be monomial. \square

Notice from this result, we can actually see that there must exist a monomial term in the singular locus purely in terms of ω , given by $\omega_{jj}\omega_{j+1,j+1}\dots\omega_{n,n}$ where $j \neq i$. This means that no matter what we set the λ values equal to, the singular locus will always be nonzero. This is also true of the simple path model. This leads us to the following proposition.

Proposition 5.7. Let G be a single path with zero or more bidirected edges somewhere along the path. Then the model has a term in the singular locus purely in ω .

We note from Theorem 7.3 of Mathias Drton's paper [14] that we already know these models are injective because they do not contain a subgraph whose bidirected part is connected and whose directed part has a unique sink.

5.3.1 Injective does not imply monomial singular locus

We know from Drton-Foygel-Sullivant [15] that every acyclic model with no bidirected edges is injective (globally identifiable everywhere). However, injective does not imply having a monomial singular locus ideal. Consider the following example:

Example 5.8. Consider the model with edges corresponding to λ_{12} , λ_{23} , λ_{14} , λ_{43} , λ_{15} , λ_{52} . Notice that we do not have disjoint paths from source to sink. The singular locus is the variety defined by:

$$\begin{aligned} & \lambda_{52}\omega_{11}^3\omega_{44}\omega_{55}^2, \\ & \omega_{11}^3\omega_{22}\omega_{44}\omega_{55}, \\ & \lambda_{14}\lambda_{52}\omega_{11}^4\omega_{55}^2, \\ & \lambda_{12}\omega_{11}^4\omega_{44}\omega_{55} + \lambda_{15}\lambda_{52}\omega_{11}^4\omega_{44}\omega_{55}, \\ & \lambda_{14}\omega_{11}^4\omega_{22}\omega_{55} \end{aligned}$$

5.3.2 Monomial singular locus does not imply injective

We show that, in the case of an acyclic, non-simple graph, we can get a monomial singular locus, but this does not imply injective (i.e. globally identifiable everywhere).

Example 5.9. Consider the model with edges corresponding to λ_{12} , λ_{23} and bidirected edge ω_{23} . The singular locus is given by:

$$\lambda_{12}\omega_{11}^2$$

Thus setting λ_{12} to zero results in an unidentifiable model, so the model is not injective (globally identifiable everywhere).

5.3.3 Relationship between singular locus term in ω and injectivity

We saw in Example 5.8 that, although we do not get a monomial singular locus, we do have a term in the singular locus purely in terms of ω . This forces the model to be injective, as no amount of setting lambdas to numerical values will cause the entire singular locus to go to zero.

We conjecture that the converse is true as well.

Conjecture 5.10. Assume our model is injective. Then there is a monomial term solely in ω in the singular locus.

We note that an added complication here is that the term in ω may not be a minor of the reduced Jacobian, but it might be in the Groebner Basis of the minors of the reduced Jacobian. This is the case in Example 5.8, as there is no minor that is purely in ω , but when we find a Groebner Basis of all the minors, we get a term purely in ω .

Conclusion

This thesis contains algebraic and combinatorial applications to three biologically inspired problems: chemical reaction networks with binomial steady-states, phylogenetic consensus trees as tropical Fermat-Weber points, and linear structural equation models given by acyclic mixed graphs.

The first main result, Theorem 3.12, concerns the mixed volume of partitionable binomial networks whose steady-states are defined by two sets of polynomials: binomials f_1, \dots, f_{n-d} and linear polynomials $\mathbf{w}_i \mathbf{x} - c_i$ for $i = n - d + 1, \dots, n$. The main result states that the mixed volume of $\sum_i \text{Newt}(f_i) + \sum_i \text{Newt}(\mathbf{w}_i \mathbf{x} - c_i)$ is the volume of at most one mixed cell – a higher dimensional parallelogram whose volume can be computed by a matrix determinant. This result arises because of the geometry of the linear span of \mathbf{w}_i (the space of conservation laws) and polytopes $\text{Newt}(f_i)$. Specifically, partitionability of the network assumes that the affine hull of $\text{Newt}(f_i)$ is orthogonal to the space of conservation laws. The main result is then applied to a one parameter family of partitionable binomial cycle networks and show that their mixed volume is depends on the parity of the number of vertices, or complexes, in the cycle.

To further applicability of this mixed volume result, we expect some gen-

eralizations can be made. First, the proof of this result requires that the conservation law vectors \mathbf{w}_i be disjoint 0/1-vectors. We suspect that the disjoint condition can be removed since the choice of edges defining mixed cells in any subdivision are required to be linearly independent. However, our proof relies on the disjoint condition. Another method to extend the use of Theorem 3.12 is to “nearly” partitionable binomial networks. For instance, the Edelman network was shown to be a non-example of a partitionable network in Example 3.7. However, it can be shown that a slight modification of this network is partitionable and has the same mixed volume. Even though the Edelman network is not binomial, we expect that this can be done for binomial networks that are not partitionable.

The second problem addressed in this thesis is phylogenetic consensus trees. Specifically, given tree metrics $\mathbf{v}_1, \dots, \mathbf{v}_n$ and weights w_1, \dots, w_n , find an optimal point \mathbf{v}^* which minimizes the weighted sum of distances $\mathbf{d}(v^*, v_i)$ for the tropical asymmetric metric \mathbf{d} . Under this formulation of the problem, a consensus tree is an optimal point of this sum. In other areas of research, these optimal points are known as Fermat-Weber points. In Chapter 4, the main result, Theorem 4.28, states that any cell of the regular subdivision of Cayley polytope induced by the weights w_i can correspond to the set of Fermat-Weber points. The proof of this theorem relies on two established results: the Cayley trick and a result which gives a correspondence between subsets of vertices of a product of simplices and subgraphs of a complete bipartite graph.

The third application in this thesis is to linear structural equation models given by acyclic mixed graphs. First we describe the singular locus ideal for

directed star graphs G with inward and outward arrows, Theorems 5.2 and 5.3. In both cases, the polynomials are obtained as certain minors of the Jacobian of the covariance parameterization map ϕ_G and these polynomials can be combinatorially described in terms of G . Lemma 5.5 also shows that if G is a disjoint union of directed paths, then the Jacobian can be reduced to a block diagonal matrix. In this case, the minors can be more easily seen even without the use of computer algebra. This result is later applied to the case of a single path with some bidirected edges to show that its singular locus ideal is monomial – this is the content of Proposition 5.6. For future work, we are interested to see the effect on the reduction of the Jacobian for path disjoint directed graphs if we glue together a pair of sources vertices or a pair of sink vertices. For instance, directed star graphs with outward arrows can be obtained by consecutively gluing source vertices of pairs of directed edges.

Bibliography

- [1] Carlos Brito and Judea Pearl. Generalized instrumental variables. 2002.
- [2] David Bryant. A classification of consensus methods for phylogenetics. *DIMACS series in discrete mathematics and theoretical computer science*, 61:163–184, 2003.
- [3] Tianran Chen. Unmixing the mixed volume computation. *Discrete & Computational Geometry*, 62(1):55–86, 2019.
- [4] Dietmar Cieslik. *Shortest connectivity: an introduction with applications in phylogeny*, volume 17. Springer Science & Business Media, 2004.
- [5] Andrei Comănesci and Michael Joswig. Tropical medians by transportation. *Mathematical Programming*, pages 1–27, 2023.
- [6] Carsten Conradi, Elisenda Feliu, Maya Mincheva, and Carsten Wiuf. Identifying parameter regions for multistationarity. *PLoS computational biology*, 13(10):e1005751, 2017.
- [7] Jane Ivy Coons, Mark Curiel, and Elizabeth Gross. Mixed volumes of networks with binomial steady-states. *arXiv preprint arXiv:2303.18096*, 2023.

- [8] David Cox, John Little, Donal O’shea, and Moss Sweedler. *Ideals, varieties, and algorithms*, volume 3. Springer, 1997.
- [9] Shelby Cox and Mark Curiel. The tropical polytope is the set of all weighted tropical fermat-weber points. *arXiv preprint arXiv:2310.07732*, 2023.
- [10] Jesús De Loera, Jörg Rambau, and Francisco Santos. *Triangulations: structures for algorithms and applications*, volume 25. Springer Science & Business Media, 2010.
- [11] Alicia Dickenstein. Biochemical reaction networks: An invitation for algebraic geometers. In *Mathematical congress of the Americas*, volume 656, pages 65–83. Contemp. Math, 2016.
- [12] Alicia Dickenstein, Mercedes Perez Millan, Anne Shiu, and Xiaoxian Tang. Multistationarity in structured reaction networks. *Bulletin of Mathematical Biology*, 81:1527–1581, 2019.
- [13] Zvi Drezner and Horst W Hamacher. *Facility location: applications and theory*. Springer Science & Business Media, 2004.
- [14] Mathias Drton. Algebraic problems in structural equation modeling. In *The 50th anniversary of Gröbner bases*, volume 77, pages 35–87. Mathematical Society of Japan, 2018.
- [15] Mathias Drton, Rina Foygel, and Seth Sullivant. Global identifiability of linear structural equation models. *Annals of statistics*, 39(2):865–886, 2011.

- [16] Timothy Duff, Cvetelina Hill, Anders Jensen, Kisun Lee, Anton Leykin, and Jeff Sommars. Solving polynomial systems via homotopy continuation and monodromy. *IMA Journal of Numerical Analysis*, 39(3):1421–1446, 2019.
- [17] Elizabeth Gross, Nicolette Meshkat, and Anne Shiu. Identifiability of linear compartmental models: The singular locus. *Advances in Applied Mathematics*, 133:102268, 2022.
- [18] Robin Hartshorne. *Algebraic geometry*, volume 52. Springer Science & Business Media, 2013.
- [19] Fritz Horn and Roy Jackson. General mass action kinetics. *Archive for rational mechanics and analysis*, 47:81–116, 1972.
- [20] Birkett Huber, Jörg Rambau, and Domingo Gómez-Pérez. The Cayley trick, lifting subdivisions and the Bohne-Dress theorem on zonotopal tilings. *Journal of the European Mathematical Society*, 2(2):179–198, 2000.
- [21] Birkett Huber and Bernd Sturmfels. A polyhedral method for solving sparse polynomial systems. *Mathematics of computation*, 64(212):1541–1555, 1995.
- [22] Badal Joshi and Anne Shiu. Which small reaction networks are multistationary? *SIAM Journal on Applied Dynamical Systems*, 16(2):802–833, 2017.
- [23] Michael Joswig. *Essentials of tropical combinatorics*, volume 219. American Mathematical Society, 2021.

- [24] Diane Maclagan and Bernd Sturmfels. *Introduction to tropical geometry*, volume 161. American Mathematical Society, 2021.
- [25] Adam Mahdi, Antoni Ferragut, Claudia Valls, and Carsten Wiuf. Conservation laws in biochemical reaction networks. *SIAM Journal on Applied Dynamical Systems*, 16(4):2213–2232, 2017.
- [26] Yurii Nesterov. *Introductory lectures on convex optimization: A basic course*, volume 87. Springer Science & Business Media, 2013.
- [27] Nida Obatake, Anne Shiu, and Dilruba Sofia. Mixed volume of small reaction networks. *Involve, a Journal of Mathematics*, 13(5):845–860, 2020.
- [28] Lior Pachter and Bernd Sturmfels. *Algebraic statistics for computational biology*, volume 13. Cambridge University Press, 2005.
- [29] Mercedes Pérez Millán, Alicia Dickenstein, Anne Shiu, and Carsten Conradi. Chemical reaction systems with toric steady states. *Bulletin of mathematical biology*, 74:1027–1065, 2012.
- [30] Francisco Santos. The Cayley trick and triangulations of products of simplices. *Contemporary Mathematics*, 374:151–178, 2005.
- [31] Bernd Sturmfels. On the newton polytope of the resultant. *Journal of Algebraic Combinatorics*, 3:207–236, 1994.
- [32] Bernd Sturmfels. *Solving systems of polynomial equations*. Number 97. American Mathematical Soc., 2002.

- [33] Seth Sullivant. *Algebraic statistics*, volume 194. American Mathematical Soc., 2018.
- [34] Seth Sullivant, Kelli Talaska, and Jan Draisma. Trek separation for Gaussian graphical models. *The Annals of Statistics*, 38(3):1665 – 1685, 2010.
- [35] Jan Verschelde. Homotopy methods for solving polynomial systems tutorial at ISSAC'05, Beijing, China, 24 July 2005.
- [36] Ruriko Yoshida and Shelby Cox. Tree topologies along a tropical line segment. *Vietnam Journal of Mathematics*, 50(2):395–419, 2022.